Journal of Controlled Release 371 (2024) 216–236

Contents lists available at ScienceDirect

Journal of Controlled Release

journal homepage: www.elsevier.com/locate/jconrel

Review article

To see or not to see: *In vivo* nanocarrier detection methods in the brain and their challenges

Antonia Clarissa Wehn [a,b], Eva Krestel [a], Biyan Nathanael Harapan [a,b], Andrey Klymchenko [c], Nikolaus Plesnila [a,d], Igor Khalin [a,e,*]

[a] Institute for Stroke and Dementia Research (ISD), Munich University Hospital, Feodor-Lynen-Straße 17, 81377, Germany
[b] Department of Neurosurgery, University of Munich Medical Center, Marchioninistraße 17, 81377 Munich, Germany
[c] Laboratoire de Biophotonique et Pharmacologie, CNRS UMR 7213, Université de Strasbourg, 74 route du Rhin - CS 60024, 67401 Illkirch Cedex, France
[d] Munich Cluster of Systems Neurology (SyNergy), Feodor-Lynen-Straße 17, 81377 Munich, Germany
[e] Normandie University, UNICAEN, INSERM UMR-S U1237, Physiopathology and Imaging of Neurological Disorders (PhIND), GIP Cyceron, Institute Blood and Brain @ Caen-Normandie (BB@C), 14 074 Bd Henri Becquerel, 14000 Caen, France

ARTICLE INFO

Keywords:
Nanoparticles
Blood-brain barrier
Detection
Biodistribution
In vivo

ABSTRACT

Nanoparticles have a great potential to significantly improve the delivery of therapeutics to the brain and may also be equipped with properties to investigate brain function. The brain, being a highly complex organ shielded by selective barriers, requires its own specialized detection system. However, a significant hurdle to achieve these goals is still the identification of individual nanoparticles within the brain with sufficient cellular, subcellular, and temporal resolution.

This review aims to provide a comprehensive summary of the current knowledge on detection systems for tracking nanoparticles across the blood-brain barrier and within the brain. We discuss commonly employed *in vivo* and *ex vivo* nanoparticle identification and quantification methods, as well as various imaging modalities able to detect nanoparticles in the brain. Advantages and weaknesses of these modalities as well as the biological factors that must be considered when interpreting results obtained through nanotechnologies are summarized. Finally, we critically evaluate the prevailing limitations of existing technologies and explore potential solutions.

1. Introduction

In recent years, nanotechnology has gained increasing popularity in the neurosciences due to its versatility and capability to adapt to specific and individual requirements. Nanocarriers not only safeguard transported molecules from degradation but also provide precise control over their release across both time and space [1–3]. Thus, they find significant utility in diverse applications such as fluorescent labeling [4–6], contrast enhancement [7,8] and targeted drug delivery [9–12]. Their unique ability to interact with cells at the nanoscale level give them a distinct advantage over conventional macro-molecular substances [13]. Nonetheless, despite the widespread use of nanotechnologies in various industrial and consumer products [14,15], their application in the biological and medical field is subject to many specific challenges [16]. Particularly when targeting the brain, only a tiny fraction of injected particles can successfully reach the target site, and the proportion of nanocarriers found in the brain compared to other organs is generally low [17]. For instance, nanocarriers targeting the liver may exhibit an uptake rate of 30–99% when systemically administered [18,19], whereas brain uptake ranges from 0.01% to 0.5% [20–22]. The use of nanotechnologies for the treatment of various brain pathologies such as tumors [23–25], Alzheimer's disease [26–28], ischemic stroke [29,30] and traumatic brain injury (TBI) [31–33] has been promising experimentally, and few brain-targeting nanocarriers are currently undergoing advanced clinical trials [34–36]. However, no active brain targeting nanocarrier is currently available on the market.

1.1. Brain barriers and their role in drug delivery

The central nervous system (CNS) consists of multiple compartments such vessels, parenchyma, or cerebrospinal fluid (CSF), each separated by specific barriers: the blood-brain barrier (BBB) (Fig. 1A), the blood-

* Corresponding author at: Feodor-Lynen-Straße 17, 81377 Munich, Germany.
E-mail addresses: antonia.Wehn@med.uni-muenchen.de (A.C. Wehn), eva.krestel@med.uni-muenchen.de (E. Krestel), biyan.harapan@med.uni-muenchen.de (B.N. Harapan), andrey.klymchenko@unistra.fr (A. Klymchenko), Nikolaus.Plesnila@med.uni-muenchen.de (N. Plesnila), igor.khalin@inserm.fr (I. Khalin).

https://doi.org/10.1016/j.jconrel.2024.05.044
Received 16 February 2024; Received in revised form 18 May 2024; Accepted 23 May 2024
Available online 31 May 2024

CSF barrier (Fig. 1B), the blood-arachnoid barrier (Fig. 1C), and the CSF-brain barrier (Fig. 1D). A basic understanding of these compartments and barriers is needed when aiming to detect nanocarriers, since the biodistribution of NPs is a highly dynamic process, and particle accumulation within any of the aforementioned compartments is possible. Thus, both spatial and temporal information are key to properly interpreting particle behavior and assessing clinical relevance.

The BBB is a functional entity on the level of cerebral capillaries which regulates passage from the blood to the brain, preventing the entry of potentially harmful blood-derived molecules into the brain parenchyma [37–39]. Tight junctions between capillary endothelial cells create a physical barrier, thereby upholding the paracellular impermeability of the BBB. In addition, the transcellular impermeability of the BBB is further reinforced by the activity of membrane efflux pumps [40,41] as well as the specialized lipid composition of the endothelial cell-membrane. This lipid arrangement minimizes the formation of caveolae invaginations [42], reducing nonspecific endocytosis in brain endothelial cells. These characteristics of the BBB pose a significant challenge for delivering therapeutic substances to the brain. Under pathological conditions, however, loss of BBB integrity is a commonly observed feature and may therefore facilitate drug delivery [43]. For instance, alterations in endocytic rates can significantly impact BBB integrity, even in the presence of intact tight junctions due to increased levels of transcytotic vesicles [44], also contributing to the compromised BBB function observed in conditions such as aging [45] or acute stroke [46].The proper distinction between healthy and injured conditions is therefore imperative when conducting pharmacological research on the BBB. However, even in pathology, small molecule therapeutics cannot sufficiently cross the BBB, suggesting the involvement of complex restriction mechanisms. Consequently, there is a need for further characterization of the pathophysiological processes of the BBB to uncover therapeutic accessibility to the brain and develop novel strategies.

Various *in vitro* BBB models have been developed to date, *i.e.* CNS organoids [47], 3D vascular cultures [48,49] or BBB-on-chip [50] which aim to mimic transendothelial transport. Unfortunately, current methods are still unable to fully replicate the dynamic complexity of delivery processes *in vivo*. Pharmacokinetic parameters such as biodistribution, elimination, shear forces, opsonization or off-target compartmentalization cannot be adequately reproduced *in vitro*. Drug effects demonstrated using *in vitro* BBB models are usually hard to replicate *in vivo* due to the limited knowledge about the final concentration of the compound in the target organ or high adverse reactions, especially in the liver or spleen. Therefore, for final validation, studies should be conducted on the entire living organism. This is especially critical in the context of brain targeting, where drug penetration through the BBB is severely limited. This review therefore focuses specifically on the *in vivo* application of nanocarriers.

1.2. Nanoparticles as theranostic agents

Apart from drug-delivery, nanoparticle-based technologies have achieved a significant milestone by serving as detectors, enabling a better understanding of cellular and subcellular processes, particularly in monitoring the transmigration of various molecules and substances across the BBB [51,52]. Due to their small size and high versatility, NPs not only enhance the spatial resolution of imaging technologies [53,54] but also enable real time visualization of dynamic processes *in vivo* [55,56]. Conventional fluorescent *ex vivo* and intravital imaging is often limited to visualization in cellular resolution. NPs loaded with contrast agents provide a higher resolution of biological processes when combined with well-established imaging modalities such as multi-photon imaging [57], magnetic resonance imaging (MRI) [58,59] or X-ray computed tomography (CT) [60]. Their surface can be functionalized with a wide range of ligands [61], including but not limited to polyethylene glycol (PEG), peptides, antibodies, deoxyribonucleic acid (DNA) [62], ribonucleic acid (RNA) aptamers *etc.* This ensures stealth properties and the ability to target tissues of interest or to detect biomolecules. Nevertheless, detecting and visualizing low concentrations of NPs in target tissues or even individual particles remains a significant

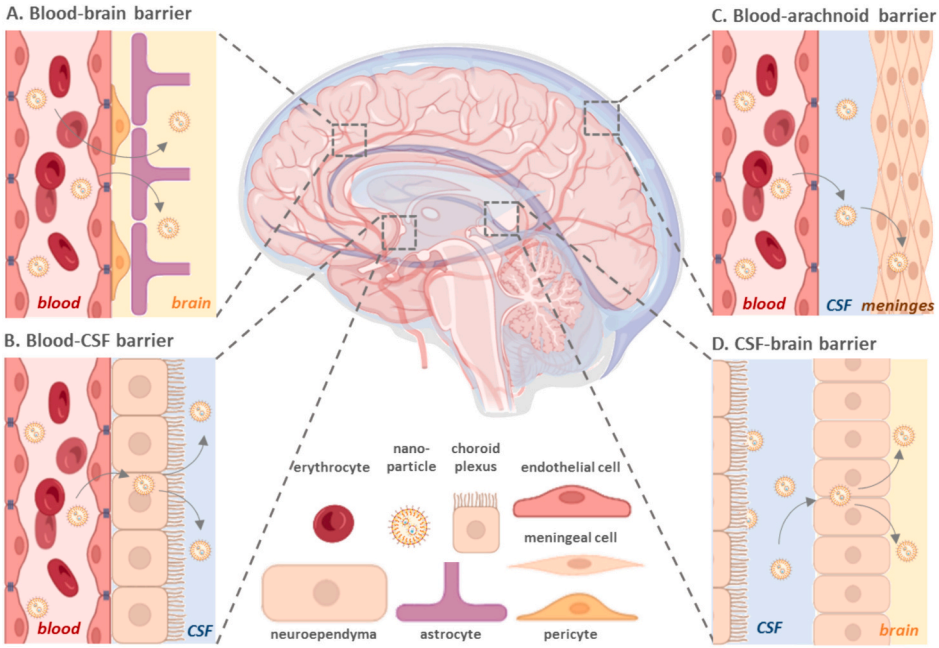

Fig. 1. Visualization of different compartments and barriers within the central nervous system (CNS). A. Blood-brain barrier (BBB): the BBB is composed of the endothelial vessel wall, connected by tight junctions, as well as pericytes and astrocyte end-feet. NPs can cross from the vessel lumen into the brain parenchyma. B. Blood- cerebrospinal fluid (CSF) barrier: the blood-CSF barrier links the blood stream to the CSF compartments of the CNS. NPs can therefore enter the CSF stream and be cleared from the brain. C. Blood-arachnoid barrier: the blood-arachnoid barrier removes drugs from the brain tissue by transporting them from the cerebrospinal fluid (CSF) to the meningeal lymphatic vessels; D. CSF-brain barrier: The CSF-brain barrier separates the brain parenchyma from the surrounding CSF. NPs can stay in brain endothelial cells, exit the CSF stream and distribute within the brain parenchyma. Created with BioRender.com.

challenge (Fig. 2).

In this review, we aim to provide a summary of recent pre-clinical developments specifically in detection modalities based on nanocarriers within the context of the CNS, while discussing their challenges and potential implications. We differentiate between functional, quantitative and qualitative detection methods and discuss their respective advantages and limitations, with a concise summary provided in Table 1.

2. Detection methods

2.1. Functional assessments: animal behavior and survival to validate drug delivery across the BBB

One of the earliest approaches to evaluate whether nanocarriers crossed the BBB was *via* the CNS effect of the transported drug (pharmacodynamics) detected by changes in animal behavior [63–65] (Table 1 A). Behavioral readouts reflect the function of the CNS with high levels of versatility, despite being prone to experimental bias. One of the first examples was the use of loperamide [66], which is an opioid receptor agonist, also known as Imodium®, primarily acting on μ-opioid receptors of the peripheral nervous system (PNS) to reduce diarrhea [67]. In contrast to other opioids, *i.e.* morphine, loperamide has a limited capability to cross the BBB due to efflux by P-glycoprotein [68]. Encapsulation of loperamide in polysorbate coated poly(butyl cyanoacrylate) particles enhanced BBB crossing in healthy mice by measuring the drug's analgesic effect *via* the tail flick test [64]. Here, behavior was used as a proxy for increased brain penetration of nanocarriers. This same idea of using loperamide's pharmacodynamic properties to measure central analgesic efficacy has also been used as proof of principle experiment in further studies for assessing the potential of different NP cores and coatings [69,70]. This can also be done for other analgesic drugs: Yang et al. used NPs containing cobra neurotoxin with a central analgesic effect to show that brain accumulation was increased by creating red light generated reactive oxygen species which open the BBB and promote nanocapsule degradation to increase the penetration of the drug into the brain [71]. The analgesic effect is measured using the hot plate test as well as acetic acid-induced writhing and was indeed reduced in the group where neurotoxin NPs were administered. Other studies apply various NP-loaded drugs to healthy animals to induce central neurological symptoms *via* specific drug-loaded nanocarriers, such as amphetamine-induced psychosis or parkinsonism. Subsequently, they employed a range of behavioral tests, like the forced swimming test to assess depression-like behavior, activity chamber or open field tests for locomotor function, and the passive avoidance test for memory function assessment [72–76]. Such findings are usually underpinned with biochemical and histological assessments to demonstrate the biodistribution of the applied compound [77].

The functionality of a drug may also be assessed *via* behavior in various models of disease. For instance, Parkinson's disease (PD) is a progressive nervous system degenerative disorder that affects motor function [78], therefore specific behavioral tests assessing motor function are commonly used to assess drug efficacy in animal models. Kundu et al. tested curcumin and piperine delivery into the brain, both impermeable to the BBB, and evaluate motor function *via* rotarod testing in a PD mouse model. They support their findings by quantitative and qualitative biodistribution assays [79]. Rotarod testing [80,81], as well as additional spontaneous motor tests [82] or exploration tests for higher cognition [83], are often use to validate drug permeability to the brain in Parkinson's disease by an improvement in motor function after NP application. Similarly to PD, motor-functional assays may be used to assess drug efficacy in rabbit models of cerebral palsy [84,85] or animal models of Huntington's disease [86,87], both diseases that primarily affect motor function.

Other brain pathologies such as Alzheimer's disease (AD) focus more on neurocognitive assays. For instance, several studies use cognitive

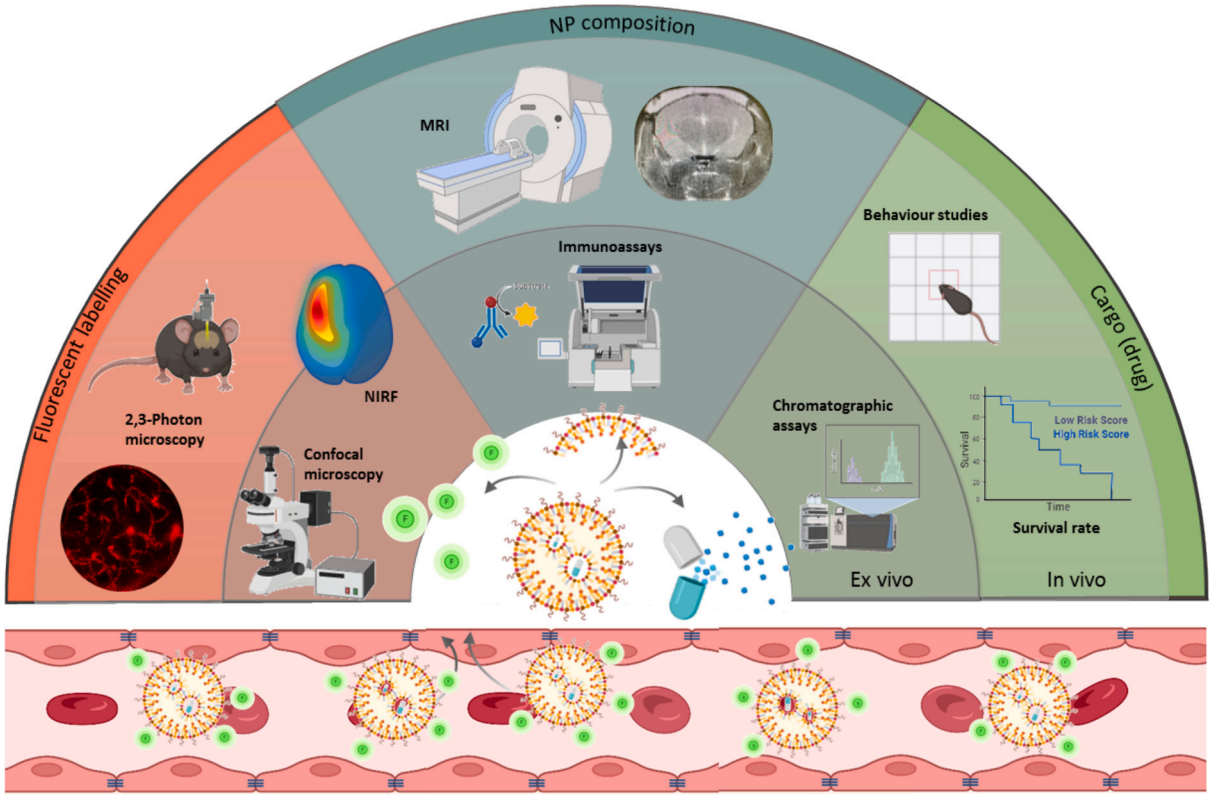

Fig. 2. Schematic overview of commonly used detection modalities of nanoparticles for BBB permeability.
NIRF: near-infrared fluorescence; MRI: magnetic resonance imaging, NP: nanoparticle. Created with BioRender.com.

Table 1
Summary of nanoparticle-related studies and reports sorted by the type of assessment.

	Type of assessment	references	BBB, disease, and size of NPs		
A. Functional assessment: validation of drug delivery across the BBB	**Behavioral studies** (including memory and motor functions)	[31,63–66,69–77,79–98]	healthy / intact BBB		• < 100 nm [73–77,83] • 100–200 nm [76,77] [64,86] • > 200 [63, 65, 66, 69, 71, 72, 77]
			pathological BBB	Alzheimer's Disease	• < 100 nm [89,91,95] • 100–200 nm [88,93,94,96] • > 200 nm [92,97]
				Parkinson's Disease	• < 100 nm [79,82,83] • 110–200 nm [80,81]
				others	• Cerebral palsy, 3.2 nm ± 0.4 nm – 21.0 nm ± 1 nm [85] • Cerebral palsy, 8.5 nm [84] • Huntington's Disease, particle size not stated [87] • Huntington's Disease, < 200 nm [86] • Cerebral ischemia (middle cerebral artery occlusion), 50 nm [98] • Glioma, 167 nm, 290 nm [69] • Pentylenetetrazole induced cognitive impairment, 157.1 ± 3.7 nm – 528.2 ± 1.9 nm [90] • Traumatic brain injury, 220 nm [31]
	Survival studies	[100–112]	healthy / intact BBB		• < 100 nm [100,101,104,105,108] • 100–200 nm [102,105,107,109] [103,107,110,111] • 100–200 μm (microparticle) [106]
			pathological BBB	Glioma	
				Brain metastases from breast cancer	• 145.2 nm [112]
B. Quantitative assays: concentration levels in functional tissue translate BBB permeabilization	**Chromatographic essays** (including mass spectrometry)	[122–162,171–180,182–184,186–206]	healthy / intact BBB		• particle size not stated [152] • < 100 nm [126,127,129,137,147,148,151,161,162,184,186,188,191,196,200,203] [159,171,204] • 100–200 nm [122–125,132–136,139,141,143,146,148,155,156,179,187,189,190,194,195,203,206] • > 200 [123, 128, 131, 143, 145, 173, 197–199, 201] • 4–5 μm [193]
			pathological BBB	Glioma	• < 100 nm [150,154,175] • 100–200 nm [140,144,158,177,178,205] • > 200 [158, 180]
				Cerebral ischemia (*e.g.*, middle cerebral artery occlusion)	• 71 ± 9.5 nm [160] • 139 nm [202] • 143.6 ± 6.7 nm [174]
				others	• Breast cancer metastases, 40 nm [182] • Breast cancer metastases, 140 nm [138] • Parkinson's Disease, 75.37 ± 3.37 nm [192] • Parkinson's Disease, 164 ± 3 nm [142] • HIV-1 encephalitic mouse model, < 200 nm [130] • Temporal lobe epilepsy, 1.1 nm [149] • Epilepsy, 20 nm [172] • Cerebral palsy, 4.2–4.4 nm [183] • Diabetic cerebral infarction, 89 ± 23 nm [157] • SOD1 mutated rats (neurodegeneration characteristics), < 80 nm [176] • Paraoxon-poisoned rats, 100 nm [124]

(*continued on next page*)

Table 1 (*continued*)

	Type of assessment		references	BBB, disease, and size of NPs		
C. Qualitative and quantitative imaging modalities: localization and distribution patterns of nanocarriers for spatio-temporal evaluation	**Immunoassays (ELISA)** (occasionally in combination with IHC)		[31,163–165,181,209,268,405]	healthy / intact BBB		• particle size not stated [181] • 80 nm [406] • 342 ± 23.5 nm [405]
				pathological BBB		• Glioma, 83.82–91.56 nm [268] • Glioma, 185.0 ± 3.0 nm [165] • Cerebral ischemia (middle cerebral artery occlusion), 95 nm [163] • Parkinson's Disease, 220.1 ± 11.2 nm [164] • Traumatic brain injury, 220 nm [31] • Metachromatic leukodystrophy, 100–310 nm [209]
	PCR assays		[109,165,166,170,213,407]	healthy / intact BBB		–
				pathological BBB	Glioma	• particle size not stated [407] • 100 nm [213] • 100–150 nm [109] • 185.0 ± 3.0 nm [165]
					others	• Cerebral ischemia (middle cerebral artery occlusion), 106 ± 9.84 nm and 128 ± 7.65 nm [166] • Spinal muscular atrophy, particle size not stated [170]
	MRI-based multimodal imaging (including SPIONs/USPIO/MPIO; occasionally in combination with PET or SPECT)		[58,59,166,211–218,224–226,240–249,408]	healthy / intact BBB		• 110 and 143 nm [244]
				pathological BBB	Glioma	• < 100 nm [58,213,240–243,246,247,249] [245,409] • 100–211 nm [213,242] [214,215,224,225,245,408,410]
					Cerebral ischemia (*e.g.*, middle cerebral artery occlusion)	• 5 nm [59] • 106 ± 9.84 nm and 128 ± 7.65 nm [166] • 212 ± 1 nm [211]
					others	• Traumatic brain injury, 40 nm [212] • Traumatic brain injury, 80 nm [218] • Melanoma brain metastasis, 274 nm [216] • Intracranial tumors, < 100 nm [217] • Intracranial hemorrhage, 120 nm [411] • Temporal lobe epilepsy, 10–20 nm [226] • Parkinson's Disease, 313.5–495.4 nm [248] • Alzheimer's Disease, 263.1 nm [412]
	Fluorescence imaging and fluorescent NPs	Non-invasive *in vivo* fluorescence macro-imaging	[89,93,100,129,144,242,253–282,284,289–293,413]	healthy / intact BBB		• particle size not stated [254] • < 100 nm [129,253,255,260,263,414] • 100 nm – 200 nm [256,258,259,264,265,267] • > 200 nm [257,262,282]
				pathological BBB	Glioma	• < 100 nm [100,242,261,268,269,271,289,292,293] • 100–161 nm [144,242,270,271,290,291] • 951.37 ± 110.32 nm [415]
					Alzheimer's Disease	• 35 nm – 100 nm [89,275,277] • 100 nm – 170 nm [93,276–281]
					Cerebral ischemia (*e.g.*, middle cerebral artery occlusion)	• 27.96 ± 0.77 nm and 31.52 ± 0.82 nm [274] • 100 nm [273] • 153.2 nm and 151.8 nm [272]
					others	• Parkinson's Disease, 222.5 nm [266] • Traumatic brain injury, 100 nm, 200 nm, 800 nm [413] • Tumor (murine mammary carcinoma), 100 nm [284]
		Ex vivo fluorescence microscopy	[262,294–336,342–344,357,416,417]	healthy / intact BBB		• Particle size not stated [322] • < 100 nm [295,303,309,310,317,320,321,332,342,416] • 100–200 nm [297,305,308,320,327,336]

(*continued on next page*)

Table 1 (*continued*)

Type of assessment	references	BBB, disease, and size of NPs		
		pathological BBB	Glioma	• > 200 nm [262,320,330,333] • < 100 nm [311,312,324,326,344] • 100–200 nm [300,313,325] • > 200 nm [298,307,329]
			Cerebral ischemia (*e.g.*, middle cerebral artery occlusion)	• < 100 nm [294,315] • 100 nm – 200 nm [343,417] • 200 nm [301]
			Alzheimer's Disease	• 100–200 nm [299,302,306] • 350 nm [304]
			Traumatic brain injury	• 4.9 nm – 50 nm [323,357] • 50 nm – 100 nm [310,314,357]
			others	• Brain metastasis of triple negative breast cancer, 126 nm [328] • Cerebral malaria, 495 ± 14.4 nm [296] • hypothermic circulatory-arrest brain injury, 6.70 nm [319] • pentylenetetrazole induced seizure, 220 ± 78 nm [316] • isoniazid-induced seizure, 130–150 nm [331] • Krabbe disease, 149 ± 6 nm – 191 ± 18 nm [318] • cerebral palsy, 3.2–4.7 nm [334] • spinal cord injury, 5.2 ± 1.3 nm [335]
***In vivo* fluorescence microscopy** (*e.g.*, intravital multi photon imaging and FRET)	[57,212,284,374,375,379,380,382,383,386,388,394–399]	healthy / intact BBB		• < 100 nm [57,374,375,379,383,388,394,397] • 100–200 nm [57,374,379,382] • > 200 nm [379] [394]
		pathological BBB		• Parkinson's Disease, 70.3 ± 1.7 nm [396] • Parkinson's Disease, 88.36 ± 1.67 nm [398] • Traumatic brain injury, 40 nm [212] • Traumatic brain injury, < 200 nm [380] • Alzheimer's Disease, 16 nm [395] • Glioma, 320 ± 84 nm [386] • Tumor (murine mammary carcinoma), 100 nm [284] • Alteration of BBB permeability (*e.g.* increase of intracellular osmotic pressure), 10–100 nm [399] • CNS tuberculosis, 50–150 nm [418]

BBB: blood-brain barrier; ELISA: Enzyme-linked immunosorbent assay; IHC: immunohistochemistry; PCR: polymerase chain reaction; MRI: magnetic resonance imaging; SPIONs: superparamagnetic iron oxide nanoparticles; USPIO: ultrasmall superparamagnetic iron oxide; MPIO: *micro-sized* particles of iron oxide; PET: positron emission tomography; SPECT: single photon emission computed tomography; NPs: nanoparticles; FRET: fluorescence resonance energy transfer.

behavioral tests to assess the permeability and therapeutic function of quercetin, a natural antioxidant, loaded into NPs in order to evaluate memory function in experimental animal models of AD [88–90]. Typically, the Morris water maze [91–94], Y maze [91,95] and novel object recognition test [96,97] are used to determine drug efficacy in AD by showing an improvement in test performance. Other examples of brain pathologies examined by behavioral testing are ischemic stroke [98] and TBI [99]. We also previously demonstrated better CNS functional outcome in traumatized mice after systemic injection of brain-derived neurotrophic factor (BDNF) conjugated with poly (lactide-*co*-glycolide) (PLGA) NPs using the Neurological Severity Score and passive avoidance tests [31].

Besides functional behavior, survival may also be used as outcome parameter to assess nanoscale drug neurotoxicity/−protection. This may help to assess drug efficacy, specifically for highly lethal neurological diseases, like cerebral palsy [84]. The most widely-used application for survival studies is in high-grade brain cancer research such as high-grade glioma or brain metastases in different animal models [100–112].

The idea to measure the changes in CNS function as evidence for NPs crossing the BBB is usually inexpensive, fast, robust, and therefore offer a good screening approach for various drug-delivery platforms. However, using behavioral outcome as a read-out for a drug's ability to penetrate the BBB has obvious limitations. Firstly, it is susceptible to many confounding factors such as the animal's individual phenotype, specifically in certain strains and using specific models of pathology. Measurements can often be subjective and should therefore be carried out in a strictly blinded manner. Moreover, the impact of the therapeutic agent on peripheral receptors (*i.e.* pain receptors) or the potential for harmful accumulation of the drug in peripheral organs could also affect animal behavior, thereby complicating the interpretation of results. Behavioral assays do not offer insight into the specific mechanism responsible for crossing of the BBB, meaning the specific sequence of events leading to the observed changes in behavior is left open for speculation, *i.e.* increase in half-life of certain coatings, enhanced BBB crossing, blockage of P-glycoprotein, action through peripheral nervous system (PNS) *etc.* When CNS pathology is present, *i.e.* in brain trauma or stroke, inherent BBB dysfunction has to be assumed when interpreting data and drawing conclusions. Moreover, behavioral studies provide no spatial information on specific accumulation within affected brain compartments relevant for the studied pathology, such as the motor cortex for assessing motor function, the substantia nigra specifically for PD or the amygdala in pain related studies. Consequently, behavior may serve as a proxy for a drug's efficiency, but needs to be complemented by further analysis to resolve its mechanistic and spatio-temporal profile, since the path between drug introduction and effect remains obscure (Fig. 3).

2.2. *Quantitative methods for analyzing nanocarrier transport across the blood-brain barrier*

Quantitative drug distribution assessment methods are useful for confirming the presence of a loaded drug within the targeted organ, *i.e.* the brain, to shed light on its kinetics within the living organism (Table 1B).

Measuring NP mass is one approach to assessing the concentration of (metallic) nanoparticles in a target sample. Various techniques, such as UV–visible spectroscopy [113], Atomic absorption spectrometry [114], Matrix-assisted Laser Desorption/Ionization Mass Spectrometry (MALDI-MS) [115–117] and inductively coupled plasma mass spectrometry (ICP-MS) [118,119] rely on direct NP mass measurement in order to ascertain tissue concentration. These methods offer distinct advantages, providing high-resolution measurements, allowing for analysis at the level of individual nanoparticles within a liquid sample. Furthermore, they do not rely on fluorescent/radioactive tags which might be altered during biological/histological processing.

In contrast, high-performance liquid chromatography (HPLC) is a method separating molecules with different binding affinities to an absorbent and commonly used to analyze a drug's concentration in a target sample with high specificity and sensitivity [120,121]. HPLC assays are standard for estimation of *in vivo* pharmacokinetics of NPs by determining plasma concentration levels of a loaded drug over time

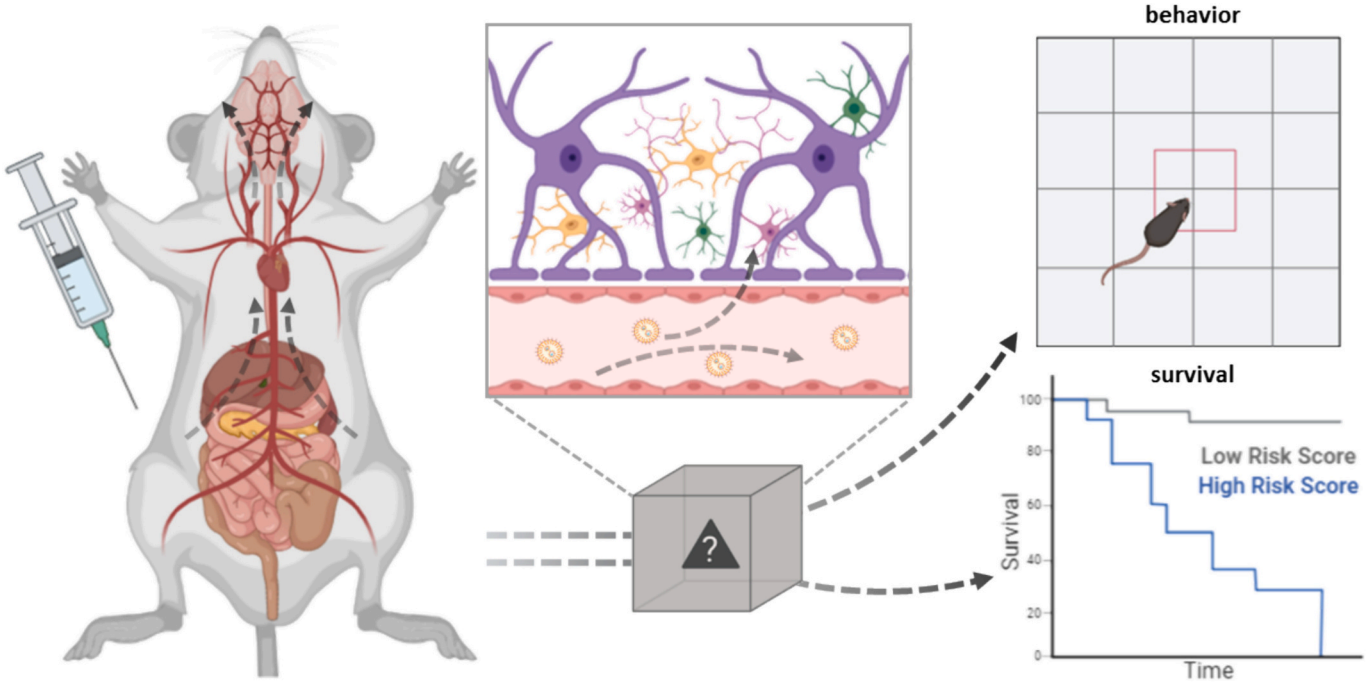

Fig. 3. Schematic of principle and problem of behavioral studies for assessment of pharmacological effect of nanocarriers in the living organism. While the drug effect or toxicity can be measured using these modalities, the path between application and effect resembles a black box and remains obscure. Created with BioRender.com.

[122–130] or biodistribution of drug-loaded nanocarriers by measuring concentrations of their components in different organs [131–137] (*i.e.* brain, liver, kidney, spleen, lungs or heart). Effectively, the pharmacological profile of nanocarriers can be determined using HPLC [138–146]. HPLC may also be used to assess BBB permeability by measuring brain concentration levels of nanocarrier components in the brain, for instance to characterize a newly developed nanocarrier [147–152] or application method such as focused ultrasound (FUS) [153,154]. More commonly, however, chromatography is used to measure the drug quantity loaded into a nanoparticle, thus allowing to also determine the releasing capabilities of the specific carrier [155–162].

Enzyme-Linked Immunosorbent Assay (ELISA) is an enzyme-based immunoassay, commonly used for the detection of target analytes in biological tissues. ELISA may be used to evaluate nanoparticle or drug concentrations in the brain after systemic administration. For instance, we previously used this approach to quantify BDNF concentrations in mice brains after application of PLGA-NP encapsulated BDNF in an animal model of TBI [31]. Similar approaches were used in nanocarrier studies assessing BDNF application after focal cerebral ischemia [163], vascular endothelial growth factor (VEGF) concentrations in an animal PD model [164] or Bevacizumab administration in a mouse glioblastoma model [165].

Finally, PCR may be used for NP distribution studies in the brain [166], for instance by measuring RNA abundance after administration of downregulating proteins or siRNA through NPs. NP technology enhances PCR quality and efficiency by improving yield, primer-DNA binding, replication, and thermal cycling [51,167]. Immuno-PCR combines the advantages of PCR and ELISA, using fluorescence-labeled oligonucleotides for heightened sensitivity [168,169]. Seo et al. quantify miRNA in glioblastoma using qtPCR after administration of anti-miRNA-loaded NPs [109]. Shabanpoor et al. measure level of full-length SMN2

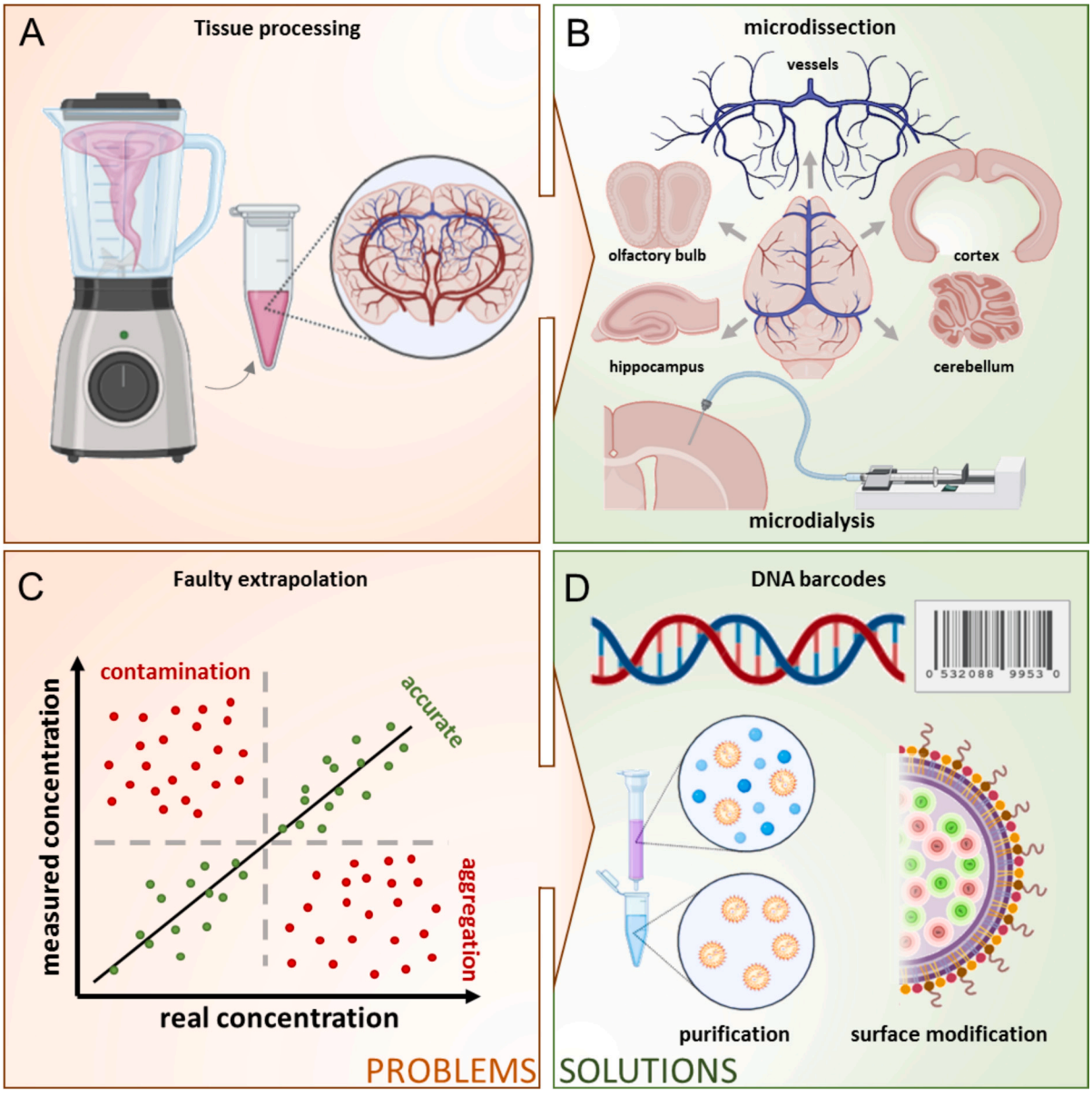

Fig. 4. Schematic overview of problems and possible solutions for quantitative assays. A. General tissue processing by homogenizing whole brain tissue does not allow to describe the localization within different brain compartments. B. Implementing microdissection of brain compartments or microdialysis helps narrow down the region of interest. C. Contamination of the sample or aggregation of fluorophores can lead to either under- or overestimation of the measured concentration. D. Implementation of additional purification processes, surface modification or selective methods such as DNA barcodes may help overcome these problems. Created with BioRender.com.

transcript after delivery of a splice-switching phosphorodiamidate morpholino oligonucleotide in a mouse spinal muscular atrophy (SMA) model [170].

While quantitative assays have become a staple in pharmacological evaluation of nanomedicine studies, limitations have to be addressed which have to be considered when analyzing data: Firstly, a significant drawback involves tissue homogenization during processing which limits exact brain localization (Fig. 4A). Recent studies have attempted to overcome these limitations by adopting a tissue compartmentalization approach, separating the brain into different tissue types such as parenchyma and endothelium [171] or different compartments such as cortex, hippocampus, cerebellum or striatum [172–176] (Fig. 4B). Moreover, in tumor studies, dividing the brain into healthy and tumorous tissue facilitates a better understanding of drug permeability. For instance, Sulheim et al. separate the brain into its tumor bearing and non-bearing hemispheres and measure drug concentration levels [177]. Others separate the brain into tumorous and non-tumorous tissue, thus determining the increase of drug accumulation at the site of the tumor and relating it to enhanced tumor uptake, hence claiming improved efficiency of either NP composition, *i.e.* coatings specifically targeting tumor cells, or application methods such as focused ultrasound (FUS) [104,178–180].

Further, beside missing information on tissue compartmentalization, quantitative assays often lack insight into precise spatial distribution at cellular or sub-cellular levels. Bode et al. merge quantitative ELISA data with qualitative immunohistochemical (IHC) stainings to investigate the blood clearance rate and *in vivo* biodistribution of labeled NPs in the brains of Wistar rats after intravenous injection [181]. They assess peptide quantity in rat brains and CSF for drug delivery, as well as liver for clearance. Immunohistochemistry (IHC) additionally provides increased spatio-temporal resolution in the brain localization of NPs.

Additionally, objective quantification and comparison of NPs across different studies remain challenging [17]. One way is to measure total NP mass, which provides no information on carrier or drug biodistribution in off-target organs or elimination pathways. Wyatt et al. address this issue in a murine model of brain metastatic breast cancer by comparing intracranial, intracardiac and intravenous application of camptothecin and measuring concentrations in tumor *vs.* healthy brain [182]. Subsequently, they determine effectiveness of BBB crossing by calculating the ratio of injected dose to concentration in the tissue (% of initial dose; %ID). Several studies use this same approach to evaluate nanocarrier pharmacokinetics [183,184]. A slightly more specific measurement can be done by forming the ratio between nanocarrier-encapsulated drug concentration levels within the plasma and the tissue of interest (*e.g.* the brain) (% ID/g of tissue) [185] and even at different time-points (%ID/time) [186–192]. This has the advantage considering plasma elimination, therefore adhering to pharmacokinetic principles, *i.e.* absorption, distribution, metabolism, and elimination. In general, standardizing biodistribution calculations will aid in objectively assess the extent of NP crossing.

Chromatography may also be used to evaluate various pharmacological applications to determine which shows the highest brain accumulation. Intranasal application bypasses the BBB as it involves drug absorption through the nasal mucosa and transportation along the olfactory and trigeminal nerve into the brain [193,194]. Nanomedicine-based studies have consequently used chromatographic techniques to compare intranasal to oral or systemic application [195–201]. Li et al. analyze NR2B9c peptide released from nanocarriers after intranasal and intravenous application at specific time-points examining specific brain region and plasma levels [202]. This combination of spatial and temporal distribution aids in understanding the pharmacokinetics and –dynamics of intranasal application. Shobo et al. use liquid chromatography in combination with mass spectrometric imaging to investigate and visualize drug localization in the brain after intranasal application [203].

Another inherent drawback of quantitative assays involves animal sacrifice at each time-point, increasing the required animal count and hindering longitudinal tracking of biochemical and physiological processes within the same animal over time. To address this, Zhu et al. elegantly use microdialysis [204,205] for continuous measurement of brain levels in the same animal over time to compare intranasal and intravenous application [206]. Their work demonstrated improved brain drug delivery *via* intranasal administration (Fig. 4B). However, microdialysis also presents several disadvantages. Firstly, it does not permit differentiating between vascular and parenchymal concentrations, limiting the spatial information. Secondly, the possibility of disrupting the vascular integrity remains, since the dialysis process creates an area around the probe in which all solutes capable of crossing the probe membrane are depleted [207]. Changes in the neurochemical milieu may affect basal levels and/or the pharmacological responsiveness of the substance under study. Lastly, microdialysis has limited time resolution ($\geq$1 min), which limits the dynamic assessment of NP biodistribution. More typically, 10-min collection periods are employed [207].

Further limitations of quantitative assays included sample dilution and contamination, affecting readout and data interpretation (Fig. 4C). Contamination in PCR assays may lead to non-specific product amplifications by incorporation of incorrect nucleotides. Further, quantitative assays fail to distinguish between bound and free peptide, which is crucial to assess drug bioavailability. In HPLC specifically, variability of endogenous growth factor levels can interfere with the level of compound carried by NPs, which is essential for data interpretation, notably in pathological conditions [31,208]. Further, using incorrect standards and controls may overestimate tissue drug release [209] (Fig. 4C). Strategies to enhance ELISA therefore involve brain vasculature perfusion with saline pre-processing to remove blood residues, sufficient blocking and thorough washing of samples, as well as using the correct standards to improve sample and result quality.

Dahlmann et al. propose a novel high throughput method for characterization of *in vivo* targeted nanocarriers by making use of specific nucleic acid barcodes [210] (Fig. 4D). These lipid barcoded NPs, when pooled and injected into live animals, allow quantitative biodistribution measurement across tissues using PCR deep sequencing. Currently, this approach is only validated for liver and lung, while its application to brain targeting holds promise for improved spatial distribution understanding.

In conclusion, quantitative assays are valuable yet limited for detecting BBB permeability. They efficiently assess biochemical processes and quantify nanocarrier-based solutions in tissues for pharmacokinetic and biodistribution studies. However, these assays have restricted ability to precisely localize nanocarriers and understand their dynamics or interactions within target tissues. While useful for proof of principle and indirect drug efficacy assessment, they lack insights into drug delivery mechanisms and tissue targeting due to the absence of spatial or temporal trajectories of NPs. Processing target tissues involves homogenization, centrifugation and separation of the biomatrix, yielding quantitative but not structural details at cellular or sub-cellular levels. Hence, these assays are often complemented by imaging techniques like fluorescent or radiographic imaging for comprehensive analysis.

2.3. Qualitative and quantitative imaging modalities: localization and distribution patterns of nanocarriers for spatio-temporal evaluation

2.3.1. MRI-based multimodal imaging

Earlier studies using MRI-based imaging modalities in NP research focused on morphological characterization post-treatment, *e.g.* lesion size after targeted drug-carriers application [166,211–214] (Table 1C). While offering longitudinal pharmacodynamic insights non-invasively, these approaches lack details on NPs' brain penetration efficacy. The subsequent evolution in nanomedicine introduced NPs as contrast agents for diagnostic use. These agents usually consist of an MRI contrast

NP core, sometimes incorporating or surrounded by targeting molecules, improving contrast *via* selective tissue accumulation. Gao et al. developed gold nanoprobes for selective glioma penetration triggered by the tumor's acidic environment and concomitant activation of MR, enabling more precise surgery [58]. Various other NP formulations have been specifically designed for contrast enhancement [215–217]. Miller et al. compared three contrast-enhancing NPs with different hydrodynamic sizes and relaxation properties to assess their uptake and retention kinetics following intravenous injection in a controlled cortical impact mouse model of TBI, assessing BBB crossing through particle accumulation within the brain tissue [218]. MRI however lacks resolution for nano-level targets and provides limited insight into molecular mechanisms of treatments, essentially underutilizing nanocarriers diagnostic potential. NP accumulation enhances signal-to-noise ratio, aiding MRI-based brain targeting, yet interpreting results requires caution since signal intensity cannot be seen in linear proportion to particle accumulation. More importantly, many brain-derived components affect MRI relaxation rates, additionally affecting data interpretation. Conti et al. devised a protocol aimed at aligning *in vivo* observations with a theoretical *in vitro* model of NPs behavior, thereby enhancing comprehension of NP dynamics and clearance in live animals. [219]. Briefly, they introduce a mathematical model capable of accurately forecasting the temporal evolution of Gadolinium-based NP distribution within the brain subsequent to BBB permeabilization induced by focused ultrasound (FUS). Initially, the researchers evaluate NP diffusion characteristics *in vitro* using agarose gel, followed by validation within the rat brain environment. This stepwise procedure enables the normalization of *in vivo* observations to raw *in vitro* data, facilitating MRI data refinement and enhancing interpretability.

Superparamagnetic iron oxide nanoparticles (SPIONs) offer promise as negative contrast agents due to their paramagnetic properties, impacting MRI *via* T1 and T2 relaxation times [220,221]. Their long blood half-life [222], easy surface modification and excellent biocompatibility [223] make them ideal for assessing BBB permeability. SPIONs serve as contrast agents and drug carriers in brain disease models like tumors [224,225] or epilepsy [226]. Optimal SPION size (10–50 nm) balances elimination and phagocytosis, thereby increasing agent half-life [227]. These ultrasmall superparamagnetic iron oxide (USPIO) NPs may prove ideal for BBB leakage or brain targeting discovery, but struggle with resolution, since even the most advanced high-resolution MRIs can so far only provide imaging within the micrometer range [228]. Aiming to increase signal and resolution, larger micro-sized contrast agents (MPIO) were developed, thereby increasing signal intensity. This however impedes the discovery of BBB permeability/targeting due to their bigger size. MPIOs enabled molecular imaging of brain vessels, demonstrated by targeting endoluminal vascular cell adhesion molecule-1 (VCAM-1) by large MPIOs to showcase acute brain inflammation in mice [229,230]. Conclusively, MPIOs are able to carry sufficiently high amounts of contrast material to induce detectable changes in MRI, while USPIOs are based on the principle of accumulation [230]. These contrast agents have been employed in various neurological pathologies, including ischemia [231,232], various neurodegenerative diseases [233,234] or brain cancer [235], with advancements in biodegradable matrix-based magnetic particles [236]. Biodegradable MPIOs show promise for clinical translation, fostering relevance for human usage.

The introduction of NPs to various imaging modalities, *i.e.* MRI, positron emission tomography (PET) or single photon emission computed tomography (SPECT) mark a significant diagnostic breakthrough in the past decade [237]. Multimodal imaging merges separate images, offering insights into NP biodistribution, cargo, and associated biochemical processes [238]. Further, the direct translation to the clinical setting makes these imaging modalities highly relevant for animal studies. Debatisse et al. use gadolinium-labeled NPs of different sizes for PET/MRI to image and quantify their transfer rate to characterize BBB permeability in a mouse ischemic stroke model treated with ciclosporin A [59]. PET offers significant improvements compared to its predecessors in terms of direct visualization of dynamic metabolic processes. However, PET's limited spatial resolution and lesion detectability pose challenges in evaluating subtle permeability changes or small regional differences, particularly for sub-molecular processes in BBB crossing, requiring cautious interpretation [239].

To address these limitations, modifications of NPs for dual imaging leverage the benefits of both PET/MRI and, for example, fluorescent imaging [240,241]. Cui et al. employ a dual-targeting strategy combining magnetic guidance and transferrin receptor-binding peptide T7 for targeted delivery in an *in vivo* orthotopic glioma mouse model, enabling tracking of brain accumulation by using fluorescence imaging, synchrotron radiation X-ray imaging and MRI simultaneously [242]. Other studies also adopt dual targeting strategies, enhancing brain pathology characterization by combining contrast enhancers like SPION or gold particles [243–246]. Others incorporate dual targeting with MRI-guided focused ultrasound to boost BBB permeability [247–249], correlating MRI data with fluorescent signals in corresponding brain areas.

Multimodal scanners merge advantages of different imaging techniques, enhancing overall quality and readout (Fig. 2). MRI offers higher resolution (25 to 100 μm) but low sensitivity, while PET provides high specificity but lower resolution (1–2 mm) [250]. The challenge is reaching the necessary resolution for quantitative and qualitative assessment of BBB penetration by NPs, which is mostly limited to organ-level detection.

2.3.2. *Fluorescence imaging and fluorescent NPs*

Fluorescent imaging offers rapid signal acquisition across various time scales [251] and allows simultaneous detection of multiplexed assays at cellular and subcellular levels using fluorophores emitting different colors [252]. Recent advancements have notably enhanced detection sensitivity, facilitating faster and easier single-molecule detection. Fluorescent labeling offers qualitative and quantitative real-time information on the target analyte, both *in vivo* and in real-time (Table 1C).

2.3.2.1. Non-invasive in vivo fluorescence macro-imaging. By far, the most popular method for live brain biodistribution and qualitative analysis is *in vivo* non-invasive fluorescence imaging. It uses a sensitive camera to detect fluorescence emission from fluorophores at a macroscopic level in whole-body living small animals, relating spatial-temporal intensities to NP biodistribution. This approach is commonly employed in nanomedicine studies to monitor real-time NP biodistribution by injecting a customized NP solution and measuring fluorescence intensity at different time-points [129,253–258] as well as brain accumulation, to test BBB permeability of a drug [259–267] (Fig. 5A). It's used notably in brain tumor studies for assessing targeted brain accumulation [100,268–271] and in ischemic stroke studies to detect changes in fluorescence intensity between affected and unaffected brain hemispheres [272–274]. Alzheimer's disease (AD) studies have also used this method to monitor NP accumulations in the brain, indicating enhanced plaque targeting and blood-brain barrier (BBB) opening and helping to understand general biodistribution in various organs and elimination rates over time [89,93,275–282].

Non-invasive *in vivo* fluorescence imaging provides quick and cost-effective biodistribution quantification, but faces limitations due to photon absorption, scattering, and auto-fluorescence in tissues, hindering accurate detection and quantification [283]. Traditional low emission wavelengths (~500 nm) like green fluorescent protein or luciferase systems can interfere with tissue auto-fluorescence, complicating signal separation from background noise. Enhancing signal-to-noise ratio involves shifting to near-infrared wavelengths and using brighter fluorescent agents like Cy5.5 and Cy7.5 encapsulated particles [284]. Advancements in near-infrared region II (NIR-II) imaging beyond 1000

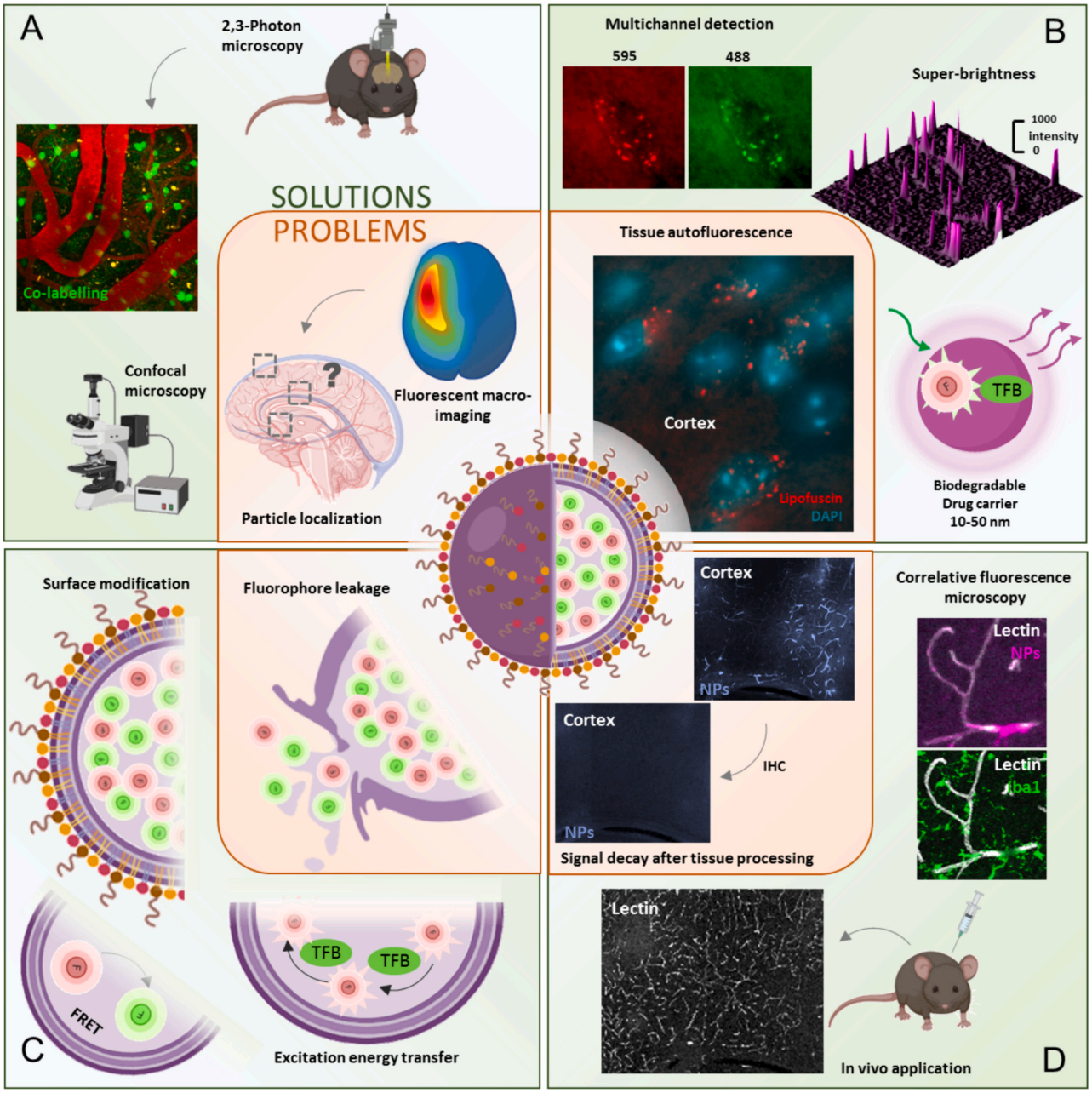

Fig. 5. Main challenges and potential solutions in fluorescent nanocarrier-based visualization modalities. A. Methods such as fluorescent macroimaging do not allow for localization of particles within brain compartments. Making use of microscopic imaging modalities such as multiphoton and confocal microscopy may offer an additional insight. B. Tissue autofluorescence from lipofuscin or neurons impedes interpretation of fluorescent signal. Therefore, using multichannel labelling might offer a possible correction pipeline. In addition, the development of ultra-bright particles may help to enable differentiation between wanted and unwanted autofluorescence. C. Fluorophore leakage due to membrane instability and overloading leads to quenching of fluorescent signaling. Surface modification and implementation of excitation energy transfer, reducing the amount of loaded fluorophores, may help to overcome this problem. D. Tissue processing for immunohistochemistry reduces fluorescent signaling by washing out particles and due to fluorescent half-life. Thus, *in vivo* application of fluorophores and immediate imaging without further tissue processing offers a more reliable approach for best fluorescent intensity measurements.

nm exhibit reduced interference with auto-fluorescence, enabling deeper tissue imaging with improved stability and sensitivity [285].

However, whole-body fluorescence imaging lacks cellular/subcellular scale resolution [250], impeding precise evaluation of NP biodistribution within specific brain compartments (Fig. 1) or understanding BBB targeting mechanisms (Fig. 5A). Moreover, beyond the inherent challenges associated with detecting and distinguishing NPs within various compartments of the brain, it is imperative to consider the mechanisms governing their clearance and potential shifts between compartments. Notably, transport proteins like LRP1 play a pivotal role in shuttling substances like Aβ and other LRP1-targeted nanocarriers from the brain into the bloodstream for metabolic processing [286,287]. Therefore, remaining cognizant of the possibility of NP translocation from one compartment to another within the observation period is paramount. Shi et al. enhanced BBB penetration by creating angiopep-2 peptide-decorated chimaeric polymersomes (ANG-CP) as a nontoxic and brain-targeting non-viral vector to boost the RNAi therapy for human glioblastoma *in vivo* [288]. Their research demonstrates the remarkable capacity of ANG-CP for BBB transcytosis, evident through a substantially elevated efflux ratio of 2.4 compared to 1.0 in

control counterparts, likely mediated *via* LRP-1 overexpressed on brain capillary endothelial (bEnd.3) cells. Notably, Shi et al. utilized bioluminescence imaging to discern and quantify this augmented BBB penetration, shedding light on the promising potential of ANG-CP for targeted brain delivery in therapeutic contexts. Combining *in vivo* fluorescence with *ex vivo* confocal imaging addresses this by offering more precise NP localization within tumorous tissues [242,289–293]. Yang et al. demonstrate this approach, defining the mechanism of doxorubicin-loaded NP uptake in glioma tissue by co-staining brain sections with tumor-associated macrophage markers (TAMs) [144], showing higher co-localization of their NPs with anti-inflammatory M2 macrophages compared to free doxorubicin. Consequently, non-invasive *in vivo* fluorescence imaging is valuable for capturing the dynamic accumulation of particles but require complementation of higher-resolution techniques for a comprehensive understanding of NP behavior within biological systems (Fig. 5A).

2.3.2.2. Ex vivo fluorescence microscopy. *Ex vivo* fluorescence imaging is used to further evaluate and confirm the biological behavior and localization of fluorescent nanocarriers at target sites and investigate their distribution in various tissues by measuring fluorescent intensity levels in the brain [294–296] or in different organs [297–300] by microscopy.

Assessing BBB permeability for nanoparticles by *ex vivo* fluorescence microscopy is not standardized and varies across labs. Some groups indirectly evaluate drug effect of a nanocarrier on biochemical processes in the brain. Specifically, inflammatory changes in the brain, such as reactive astrocytosis, microglia activation, and neuronal integrity, can be visualized and quantified [301,302]. A more direct method involves labeling NPs with fluorescent markers and tracking their distribution in tissues. Gonzalez-Carter et al. visualize distribution of avidin-functionalized nanomicelles (avidin-NMs) within the mouse brain after *i.v.* injection [303]. Other studies similarly use fluorescent NPs to track their localization within the brain [304–306], observed as speckle-like structures with corresponding emission parameters within the vessels or vessel wall [307,308], as well as in the surrounding parenchyma [262,309], cortex [310], brain tumor [311–313] or with unspecified localization [314–318].

Immunohistochemistry (IHC) stains cellular components to locate NPs. Reports study fluorescently-labeled NPs co-stained with neurons, microglia, and astrocytes, assessing distribution based on size and composition [319–323]. Wen et al. show fluorescent glycolipid-like NPs in tumor tissue and revealed increased vasculature permeability by staining for claudin-5, characterizing BBB breakdown [324]. To enhance visualization, combining *in vivo* fluorescent labeling and *ex vivo* immunohistochemical staining *via* co-labeling techniques may be used. Han et al. display NP localization in vessels and tumor cells after i.v. injection, suggesting brain entry through trans- or paracellular transport across the BBB [325]. Kang et al. co-stain gold NPs with CD31, an endothelial marker, and CD146, a marker of glioblastoma cells, revealing particle interactions in tumor tissue [326]. NPs can mostly be observed as speckle-like structures in brain cell bodies and their respective processes [327–330], indicating vesicular transport [331,332].

Ex vivo fluorescence imaging may also assess novel NP application methods. Jain et al. apply dye-loaded polymeric NPs and free dye to the nasal mucosa to investigate NP uptake [333]. Zhang F. et al. use *ex vivo* immunofluorescence imaging to assess different formulations of dendrimer-based NPs after intraamniotic administration for treatment of cerebral palsy in rabbit fetuses [334]. They use a unique approach based on the ability of the fetus to swallow amniotic fluid and compare intraamniotic application with oral administration, tracing NP transport across the intestinal villi and BBB to the brain vasculature. Zhang Y. et al. demonstrated brain accumulation of chemically functionalized gold NPs through intramuscular injection into the diaphragm of rats and transportation to the spinal cord and brainstem as a retrograde labeling method of motor neurons [335]. They elegantly show BBB crossing by visualizing NP signal in the phrenic nucleus of the ipsilateral injection side only. Thomson et al. study magnetic immunoliposomes' brain distribution with external magnetic force to open the BBB [336]. Their results imply that application of magnetic force leads to the extravasation of fluorescently-labeled NPs, indicating BBB opening. Similarly, sonopermeation has been shown to enable the safe and effective delivery of nanomedicine to the brain, with multimodal imaging highlighting that smaller-sized drug delivery systems more efficiently penetrate the brain, offering promising strategies for treating central nervous system disorders [337].

Ex vivo fluorescence imaging offers the highest resolution among fluorescent-based methods, enabling precise evaluation of NP distribution in various brain pathologies at organ and cellular levels using microscopy. Compared to non-invasive live fluorescence macroimaging, this system provides distinct advantages, such as high-resolution three-dimensional analysis of the entire brain or co-localization analysis by employing immunohistochemical markers for *post hoc* labeling of cellular and subcellular structures using different emission wavelengths in addition to fluorescent particles. However, some limitations must be addressed for accurate scientific interpretation. The short tissue penetration of fluorescent light due to scattering and auto-fluorescence creates high background tissue fluorescence in the brain [338] (Fig. 5B). Importantly, auto-fluorescent components in tissue, like intracellular vesicles such as endosomes, exhibit sizes (10–100 nm [339]) and emissions similar to NPs. Biomolecules like NADH, folic acid, and retinol emit light in the range of 450–500 nm, while riboflavin, flavin co-enzymes, and flavoproteins emit in the range of 520–540 nm [340]. Moreover, lipofuscin and lipofuscin-like pigments show broad auto-fluorescence (480–700 nm [341]), complicating their differentiation from fluorescently labeled nanocarriers due to similar morphology.

We propose a method to differentiate NP fluorescence from tissue auto-fluorescence by collecting signal both in the red and green channels, since the emission wavelength of auto-fluorescent emitters usually is broader compared to the specific emission of fluorophores [342]. Subtracting the auto-fluorescent signals from brain images reveals true NP signals at single-particle level. This method is recommended for widespread use to distinguish between auto-fluorescence and NPs. Similarly, Xu et al. measure vascular wall auto-fluorescence in the green channel to avoid interference with NP signals within the thrombus in a mouse ischemic stroke model [343]. Séhédic et al. suggested spectral imaging to monitor tissue auto-fluorescence, red fluorescent protein-labeled cells and NPs labeled with DiD dye, excluding interference and capturing real signals [344].

Another key challenge is detecting individual NPs smaller than 200 nm, which is below the resolution of most optical microscopes. Brighter particles may enhance signal-to-noise ratio, thus improving detection. Organic dyes used in fluorescence imaging, which have the advantage of biodegradability and low toxicity, have brightness limitations [345,346] compared to inorganic fluorescent NPs [347,348]. Inorganic NPs like quantum dots [349–351], nanodiamonds [352], and carbon dots [353] are popularly used due to their brightness. Conversely, fluorescent organic NPs made from organic dyes offer an attractive alternative, addressing challenges like poor biodegradability, potential toxicity, and limited brightness [354]. In this respect, we should highlight comprehensive reviews about current advances of dye-loaded polymeric [355] and lipidic [356] NPs, showcasing their varied optical properties, size flexibility, and potential clinical application due to their use of biodegradable materials (Fig. 5B).

Besides brightness limitations of individual particles, achieving sufficient brightness for brain-targeted detection remains difficult due to brain barriers limiting carrier penetration. Smaller particles (10–50 nm) aid tissue penetration but contain fewer fluorophores [357], whereas increasing fluorophore load risks aggregation-caused quenching [355], both counterproductive to brightness and signal acquisition. Novel

strategies, like using bulky hydrophobic counterions with ionic dyes [358,359] was shown to resolve the problems of aggregation-caused quenching and leakage of dyes in polymeric [360,361] and lipidic NPs [362], enhancing NP fluorescence significantly. We developed a super-bright lipid nanoemulsion loaded with rhodamine B and linked with fluorinated tetraphenylborate (TFB), a bulky counterion, successfully showing size-selective crossing of NPs across the BBB after brain trauma [357]. High dye loading in NPs may additionally lead to fluorophore leakage, reducing the signal further [363]. This leakage is a primary cause of signal misinterpretation, often causing false positive results in drug-delivery studies since it results in overestimation of particle amounts and reduced imaging performance due to higher cellular uptake of leaked dye [364]. Commonly used fluorophores like Rhodamine B or Atto-488 can have high leakage rates (20–68%) when loaded into liposomes [364]. Coupling fluorophores with bulky counterions like TFB or modifying them with apolar alkyl chains makes them more hydrophobic and less prone to leakage (Fig. 5C). Additionally, Forster resonance energy transfer (FRET) between encapsulated dyes can assess dye-loaded NP stability and counteract leakage. Klymchenko et al. demonstrate substantial differences in leakage between Nile Red and its hydrophobic analogue NR668 *in vivo* [365]. When assessing NP accumulation *via* fluorescence, it is important to note that measuring absolute values should be avoided. This is because the fluorescence intensity of the synthesized NP can be notably influenced by different factors such as, dye degradation, quenching or pH sensitivity [366].

Lastly, sample preparation (*e.g.* fixation, permeabilization, cutting *etc.*) can decompose fluorophores or NPs, hindering further evaluation. Detergents like Triton X-100 or Tween-20 used for cell lysis or permeabilization commonly destroy certain NPs, especially organic particles like lipidic ones [367], while inorganic particles such as those derived from metals (quantum and carbon dots, silica NPs) and organic polymeric NPs remain unaffected. Paraformaldehyde fixation may cross-link tissue molecules but not all types of NPs, leading to NP loss during tissue washing in staining procedures, hampering signal detection in fluorescent methods [368]. Scanning whole brain sections with intense laser light for prolonged periods may cause photobleaching and reduce fluorescent signals. Moreover, fixed and treated samples emit high auto-fluorescence that interferes with NP fluorescence.

To address these issues, a novel method of fluorescent correlation was recently described [357]. Briefly, the mouse brain vasculature was labeled *in vivo* by injecting fluorescent lectin before sacrificing the animal (Fig. 5D). Then confocal images of coronal sections were acquired, collecting fluorescent signal from injected NPs and lectin. This method retained maximum NP signal while preserving vascular landmarks stained with lectin. Subsequent IHC staining reduced NP signal drastically while preserving lectin signal. Scanning the IHC-stained sections and using lectin as a landmark allowed correlation of NP fluorescence with newly stained cell signals, *i.e.* microglia [357].

Finally, for precise localization of NP signals within intricated brain structures—whether nestled within the brain parenchyma, traversing the brain's vascular system, or confined within the endothelium of the BBB—Correlative Light and Electron Microscopy (CLEM) emerges as an innovative technique. CLEM integrates the capabilities of both Light Microscopy (LM) and Electron Microscopy (EM). Cellular structures are first imaged under LM, and the identical structures acquired under EM to obtain their ultrastructure. Information obtained by LM can be linked to the ultrastructure of the region of interest. This synergistic approach furnishes a structural framework for elucidating cellular behaviors. Achieving such correlation necessitates the identification of specific landmarks. These landmarks can be delineated through various means, such as laser branding, leveraging inherent anatomical features like blood vessels and cell bodies, or employing engineered markers like genetically expressed tags or nanoparticles [369]. Furthermore, recent advancements have showcased the efficacy of fluorescent lipidic NPs in delineating microthrombi nestled within cerebral capillaries. Their heightened lipidic density renders them detectable not only through confocal and two-photon microscopy but also in EM, enabling the evaluation of single nanoparticle behavior in subcellular resolution inside brain endothelial cells dynamically [357,370]. For an in-depth exploration of the latest advancements and future prospects in the realm of CLEM, readers are directed to an exhaustive review authored by Hayashi et al. [371].

TFB: tetraphenylborate; FRET: fluorescence resonance energy transfer; IHC: immunohistochemistry; NPs: nanoparticles. Created with BioRender.com.

2.3.2.3. In vivo fluorescence microscopy. *Ex vivo* brain imaging relies on tissue fixation, potentially altering temporal fluorescent signal trajectories. Intravital multi-photon imaging addresses this by providing high-resolution, real-time signal acquisition in living animals. This method offers dynamic, accurate physiological information, detailing NPs' behavior within brain tissue and their movement from vasculature.

Intravital microscopy in nanotechnologies allows detailed observation of NPs within brain tissue and their movement from vessels. Single- or multi-photon microscopy, popular for live imaging, involves excitation of administered fluorophores by photons in the live animal, collecting the emitted signal [372]. Single-photon microscopy enables fast and high-resolution live imaging acquisition based on a point-by-point scanning, but faces limitations in deeper tissue depths due to strong light scattering [373]. Rabanel et al. address this issue by utilizing zebrafishes' translucent properties, microinjecting NPs into the circulation of live zebrafish and testing different densities of PEG coatings for their BBB crossing abilities by observing characteristic speckle-like structures within vessels and some particles outside the vessel wall [374]. Chen et al. expanded this approach by microinjecting NPs into zebrafish brain, blood, and spinal cord [375]. They noted rapid NP accumulation throughout the brain but observed limited extravasation into surrounding tissue, suggesting distinct NP behaviors between systemic blood injection and brain-specific injection in live zebrafish.

2-photon microscopy (2-PM) offers increased imaging depth due to longer wavelength, minimizing tissue scattering and photodamage [376]. Multi-photon microscopy reduces scattering by exciting *in situ* fluorophores with multiple photons [377]. It also utilizes second-harmonic generation (SHG) for non-linear imaging which is more resistant to bleaching and does not saturate with higher illumination, providing unique contrasts for live cell and tissue imaging complementary to fluorescence [378]. Baghirov et al. assess mesoporous silica NP permeability across the BBB using 2-photon imaging but do not observe significant extravasation into the brain parenchyma [379]. Zinger et al. use intravital microscopy for capturing the cerebrovascular targeting of fluorescent NPs before and 24 h after TBI and NP administration [380]. To confirm the presence of NPs within the vasculature, they stained the vessel wall with collagen IV and visualized NPs both in and outside of the vasculature. Al-Ahmady et al. elegantly combine intravital 2-photon microscopy with MRI and IHC, describing a biphasic extravasation of liposomes following stroke in mice [381]. Further, to test brain-targeted receptor-mediated transcytosis, Kucharz et al. performed intravital 2-photon imaging after systemic application of transferrin receptor-targeted 135-nm liposome NPs in the brain vasculature of mice [382]. They load liposomes with Atto550 or Atto488 fluorescent dye, co-labeled the vasculature using FITC and demonstrate NP-associated punctates inside the vessel wall, as well as in the surrounding extravascular space. The authors conclude that transcytosis-mediated brain entry of NPs occurs mainly at the level of post-capillary venules as they are the point-of-least resistance in the BBB [382]. Moreover, this study demonstrated that the retention of NPs in the brain is dynamic and highly depends on clearance systems, like the paravascular glymphatic transport, which can only be evaluated through dynamic visualization systems. In our own work, we use intravital 2-PM to demonstrate real-time single particle motion and tracking in different brain compartments [57]. Ultra-bright polymeric

74-nm NPs made from biocompatible poly(methyl) methacrylate loaded by rhodamine coupled with a bulky counterion are used to show Brownian movements of the individual particles inside the subarachnoid space as well as particle extravasation through the BBB after brain injury. In a different study, we test low-dense lipoprotein-dependent receptor-mediated transport in brain capillaries and show the retention of 74 nm poloxamer 188 coated PLGA NPs inside brain endothelial cells (BECs) [342]. Further, the biodistribution of individual NPs is characterized *ex vivo* using confocal microscopy with additional co-stainings. Anraku et al. demonstrate a time-dependent distribution of their glycosylated nanocarriers using 2-PM for two hours and performed co-staining for endothelial cells, neurons, microglia, and astrocytes to elucidate particle trajectories across the BBB [383].

While intravital 2-PM provides dynamic, high-resolution, three-dimensional visualization of NP behavior and therefore gives valuable information of the particles' spatio-temporal distribution inside the brain, many factors should be considered when interpreting results, especially in order to accurately analyze BBB function in healthy and injured subjects. Firstly, the animals' physiological parameters must be considered, which are likely to influence BBB integrity and drug performance. The long exposure to anesthesia needed for intravital imaging as well as cranial window preparation might lead to BBB dysfunction [384] and may therefore be important confounding factors. Severe phototoxicity caused by 2-photon laser can cause damage of the brain and subsequent leakage of the BBB [385]. Next, interpretation of the acquired signal remains limited, since different possibilities of what can be seen could be argued: individual particles, aggregates of particles, or endosomes containing fluorophores leaked out from particles. Despite deeper penetration of the laser, imaging quality is typically restricted due to light scattering and high background auto-fluorescent signal [386], rendering NP detection outside of the vasculature difficult due to reduced imaging quality.

Finally, an important restriction of *in vivo* fluorescence microscopy is the restricted field of view, since its size is defined by anatomical limitations of the cranial window preparation. Partly, these drawbacks may be solved by the usage of non-invasive *in vivo* skull clearing techniques [387], which additionally have the advantage of preventing inflammation of the brain and maintaining regular CSF circulation, both phenomena impaired after cranial window preparation. Additionally, three-photon microscopy may significantly advance the imaging field by its use of wavelengths beyond 1200 nm and subsequent ability to penetrate much deeper into the tissue, thus enabling direct imaging of NPs biodistribution in the hippocampus, ventricles or choroid plexus [388].

For future nanomedicine approaches, Förster or fluorescence resonance energy transfer (FRET) presents new possibilities. FRET involves non-radiative energy transfer between excited donor and acceptor fluorophores through dipole coupling [389,390], only occuring when the intermolecular distance is smaller than the Förster radius, generally below 10 nm, ideal for the detection of interactions between molecules *in vivo* at nanometer scale [391]. It distinguishes intact nanocarriers from degrading ones, allowing real-time content release localization within tissue based on donor or acceptor channel signal intensity [284,392,393]. Few studies so far have implemented FRET for brain accumulation assessment in targeted drug delivery. Initial studies used FRET nanoprobes in zebrafish for BBB kinetics [394–396], followed by implementation in murine models. Liu et al. use FRET-based NPs composed of AIE luminogens and NIR dyes with enhanced three-photon near-infrared emission for a novel approach of *in vivo* brain angiography of the mouse brain vasculature [397]. FRET improves single particle signal, imaging depth, and resolution due to small fluorophore size [390]. Other studies use FRET to not only visualize the vasculature, but further assess particle degradation for potential drug release within the brain tissue in various brain pathology models [57,398–400] indicating BBB permeability. However, FRET's fragility requires careful implementation and continuous multimodal nanocarrier development for future use [401].

In summary, reliable fluorescent nanocarriers for imaging need specific attributes: adequate brightness, near-infrared excitation/emission, chemical and photo-stability, and proper surface chemistry (often PEGylation) for extended circulation and minimal non-specific interactions [402,403]. Specific tissue targeting necessitates ligands like antibodies or aptamers [404]. Nanocarriers for medical use should be non-toxic, biocompatible, and soluble in biological fluids. Standardization of NP preparation and handling is crucial for reproducibility across laboratories [365]. Studies using *in vivo/ex vivo* confocal and multiphoton imaging typically involve smaller (<100 nm) NPs, while alternative detection methods like MRI, PCR, and ELISA tend to involve larger NPs (>100 nm), as outlined in Table 1.

3. Conclusions

In recent years, many well-established detection modalities have been introduced to assess BBB permeability of nanocarriers for specific targeted drug delivery to the brain (Fig. 2). Indirect approaches, such as behavioral studies allow the assessment of drug efficacy in the brain for substances that typically struggle to reach the CNS. Quantitative assays, such as immune- and chromatographic assays, directly measure drug concentrations within the target tissue, while various imaging modalities enable evaluation of NP behavior in the living organism, both statically *ex vivo* as well as dynamically *in vivo*. Among these modalities, fluorescence imaging with nanoparticles stands out, enabling both high resolution imaging down to single-particle detection by multiphoton intravital microscopy, and whole-body imaging through near-infrared macroscopy methods. These biodistributional analyses promise advancements in sophisticated nanocarriers and contrast agents with improved detection capabilities, potentially setting new standards in nanotechnology. The ultimate objective is to identify individual particles at subcellular levels and monitor dynamic changes. Correlating different detection methods and continually advancing multimodal probes will facilitate more precise investigations at high spatial and temporal resolutions. This advancement holds the potential to yield groundbreaking insights into the pathophysiology of various brain diseases, paving the way for enhanced diagnostic and therapeutic strategies.

Funding

This research was supported by German Research Foundation, DFG grant: 457586042.

CRediT authorship contribution statement

Antonia Clarissa Wehn: Writing – review & editing, Writing – original draft, Visualization, Formal analysis, Conceptualization. **Eva Krestel:** Software, Formal analysis, Data curation. **Biyan Nathanael Harapan:** Writing – review & editing, Formal analysis, Data curation. **Andrey Klymchenko:** Writing – review & editing, Data curation, Conceptualization. **Nikolaus Plesnila:** Writing – review & editing, Visualization, Supervision, Conceptualization. **Igor Khalin:** Writing – review & editing, Writing – original draft, Validation, Supervision, Project administration, Funding acquisition, Conceptualization.

Declaration of competing interest

The authors declare no conflict of interest. During the preparation of this work, the authors used ChatGPT (Version 3.5) in order to reduce the word count of this review. After using this tool, the authors reviewed and edited the content.

Data availability

Data will be made available on request.

References

[1] K. Thakur, C. Attri, A. Seth, Nanocarriers-based immobilization of enzymes for industrial application, 3 Biotech 11 (10) (2021) 427.
[2] F. Farjadian, et al., Nanopharmaceuticals and nanomedicines currently on the market: challenges and opportunities, Nanomedicine (London) 14 (1) (2019) 93–126.
[3] J.S. Suk, et al., PEGylation as a strategy for improving nanoparticle-based drug and gene delivery, Adv. Drug Deliv. Rev. 99 (Pt A) (2016) 28–51.
[4] G. Battistelli, et al., Ultra-bright and stimuli-responsive fluorescent nanoparticles for bioimaging, Wiley Interdiscip. Rev. Nanomed. Nanobiotechnol. 8 (1) (2016) 139–150.
[5] G.A. Marcelo, et al., Magnetic, fluorescent and hybrid nanoparticles: from synthesis to application in biosystems, Mater. Sci. Eng. C Mater. Biol. Appl. 106 (2020) 110104.
[6] E. Rampazzo, et al., NIR-fluorescent dye doped silica nanoparticles for in vivo imaging, sensing and theranostic, Methods Appl Fluoresc 6 (2) (2018) 022002.
[7] X. Cai, et al., Manganese oxide nanoparticles as MRI contrast agents in tumor multimodal imaging and therapy, Int. J. Nanomedicine 14 (2019) 8321–8344.
[8] K. Wu, et al., Magnetic nanoparticles in nanomedicine: a review of recent advances, Nanotechnology 30 (50) (2019) 502003.
[9] A.Z. Wilczewska, et al., Nanoparticles as drug delivery systems, Pharmacol. Rep. 64 (5) (2012) 1020–1037.
[10] Y. Luo, et al., Dual and multi-targeted nanoparticles for site-specific brain drug delivery, J. Control. Release 317 (2020) 195–215.
[11] P. Kumari, B. Ghosh, S. Biswas, Nanocarriers for cancer-targeted drug delivery, J. Drug Target. 24 (3) (2016) 179–191.
[12] E. Garbayo, et al., Nanomedicine and drug delivery systems in cancer and regenerative medicine, Wiley Interdiscip. Rev. Nanomed. Nanobiotechnol. 12 (5) (2020) e1637.
[13] A.A. Yetisgin, et al., Therapeutic nanoparticles and their targeted delivery applications, Molecules 25 (9) (2020).
[14] Iijima, S., Helical Microtubules of Graphitic Carbon. n.d.
[15] X. Xu, et al., Electrophoretic analysis and purification of fluorescent single-walled carbon nanotube fragments, J. Am. Chem. Soc. 126 (40) (2004) 12736–12737.
[16] C. Kinnear, et al., Form follows function: nanoparticle shape and its implications for nanomedicine, Chem. Rev. 117 (17) (2017) 11476–11521.
[17] I. van Rooy, et al., In vivo methods to study uptake of nanoparticles into the brain, Pharm. Res. 28 (3) (2011) 456–471.
[18] Y.N. Zhang, et al., Nanoparticle-liver interactions: cellular uptake and hepatobiliary elimination, J. Control. Release 240 (2016) 332–348.
[19] W. Ngo, et al., Why nanoparticles prefer liver macrophage cell uptake in vivo, Adv. Drug Deliv. Rev. 185 (2022) 114238.
[20] A. Schnyder, et al., Targeting of daunomycin using biotinylated immunoliposomes: pharmacokinetics, tissue distribution and in vitro pharmacological effects, J. Drug Target. 13 (5) (2005) 325–335.
[21] Y.S. Kang, et al., Use of PEGylated Immunoliposomes to deliver dopamine across the blood-brain barrier in a rat model of Parkinson's disease, CNS Neurosci. Ther. 22 (10) (2016) 817–823.
[22] P.R. Lockman, et al., Brain uptake of thiamine-coated nanoparticles, J. Control. Release 93 (3) (2003) 271–282.
[23] S.C. Baetke, T. Lammers, F. Kiessling, Applications of nanoparticles for diagnosis and therapy of cancer, Br. J. Radiol. 88 (1054) (2015) 20150207.
[24] R.S. Riley, et al., Delivery technologies for cancer immunotherapy, Nat. Rev. Drug Discov. 18 (3) (2019) 175–196.
[25] M.A. Zaimy, et al., New methods in the diagnosis of cancer and gene therapy of cancer based on nanoparticles, Cancer Gene Ther. 24 (6) (2017) 233–243.
[26] A. Binda, C. Murano, I. Rivolta, Innovative therapies and nanomedicine applications for the treatment of Alzheimer's disease: a state-of-the-art (2017-2020), Int. J. Nanomedicine 15 (2020) 6113–6135.
[27] J. Gupta, et al., Nanoparticle formulations in the diagnosis and therapy of Alzheimer's disease, Int. J. Biol. Macromol. 130 (2019) 515–526.
[28] R. Martin-Rapun, et al., Targeted nanoparticles for the treatment of Alzheimer's disease, Curr. Pharm. Des. 23 (13) (2017) 1927–1952.
[29] X. Dong, et al., Nanomedicine for ischemic stroke, Int. J. Mol. Sci. 21 (20) (2020).
[30] H.Y. Kim, et al., Mesenchymal stem cell-derived magnetic extracellular nanovesicles for targeting and treatment of ischemic stroke, Biomaterials 243 (2020) 119942.
[31] I. Khalin, et al., Brain-derived neurotrophic factor delivered to the brain using poly (lactide-co-glycolide) nanoparticles improves neurological and cognitive outcome in mice with traumatic brain injury, Drug Deliv. 23 (9) (2016) 3520–3528.
[32] S. Sharma, et al., Intravenous immunomodulatory nanoparticle treatment for traumatic brain injury, Ann. Neurol. 87 (3) (2020) 442–455.
[33] T. Takahashi, et al., Novel neuroprotection using antioxidant nanoparticles in a mouse model of head trauma, J. Trauma Acute Care Surg. 88 (5) (2020) 677–685.
[34] H.-L. Roche, A.D. Brainshuttle, A Multiple Ascending Dose Study to Investigate the Safety, Tolerability, Pharmacokinetics, and Pharmacodynamics of RO7126209 Following Intravenous Infusion in Participants With Prodromal or Mild to Moderate Alzheimer's Disease. ClinicalTrials.gov, 2020.
[35] Inc., D.T, A Study to Evaluate the Safety, Tolerability, Pharmacokinetics, and Pharmacodynamics of DNL593 in Healthy Participants and Participants With Frontotemporal Dementia (FTD-GRN). ClinicalTrials.gov, 2021. NCT05262023.
[36] Inc., D.T, A Study to Determine the Efficacy and Safety of Tividenofusp Alfa (DNL310) vs Idursulfase in Pediatric Participants With Neuronopathic (nMPS II) or Non-Neuronopathic Mucopolysaccharidosis Type II (nnMPS II) (COMPASS). ClinicalTrials.gov, 2022. NCT05371613.
[37] R. Alyautdin, et al., Nanoscale drug delivery systems and the blood-brain barrier, Int. J. Nanomedicine 9 (2014) 795–811.
[38] G.C. Terstappen, et al., Strategies for delivering therapeutics across the blood-brain barrier, Nat. Rev. Drug Discov. 20 (5) (2021) 362–383.
[39] M. Choudhari, et al., Evolving new-age strategies to transport therapeutics across the blood-brain-barrier, Int. J. Pharm. 599 (2021) 120351.
[40] P.L. Golden, G.M. Pollack, Blood-brain barrier efflux transport, J. Pharm. Sci. 92 (9) (2003) 1739–1753.
[41] W. Loscher, H. Potschka, Blood-brain barrier active efflux transporters: ATP-binding cassette gene family, NeuroRx 2 (1) (2005) 86–98.
[42] B.J. Andreone, et al., Blood-brain barrier permeability is regulated by lipid transport-dependent suppression of caveolae-mediated transcytosis, Neuron 94 (3) (2017) 581–594 e5.
[43] M.D. Sweeney, et al., Blood-brain barrier: from physiology to disease and Back, Physiol. Rev. 99 (1) (2019) 21–78.
[44] A. Ben-Zvi, et al., Mfsd2a is critical for the formation and function of the blood-brain barrier, Nature 509 (7501) (2014) 507–511.
[45] A.C. Yang, et al., Physiological blood-brain transport is impaired with age by a shift in transcytosis, Nature 583 (7816) (2020) 425–430.
[46] D. Knowland, et al., Stepwise recruitment of transcellular and paracellular pathways underlies blood-brain barrier breakdown in stroke, Neuron 82 (3) (2014) 603–617.
[47] S. Bergmann, et al., Blood-brain-barrier organoids for investigating the permeability of CNS therapeutics, Nat. Protoc. 13 (12) (2018) 2827–2843.
[48] M. Campisi, et al., 3D self-organized microvascular model of the human blood-brain barrier with endothelial cells, pericytes and astrocytes, Biomaterials 180 (2018) 117–129.
[49] F. Sivandzade, L. Cucullo, In-vitro blood-brain barrier modeling: a review of modern and fast-advancing technologies, J. Cereb. Blood Flow Metab. 38 (10) (2018) 1667–1681.
[50] I. Raimondi, et al., Organ-on-A-Chip in vitro models of the brain and the blood-brain barrier and their value to study the microbiota-gut-brain axis in neurodegeneration, Front. Bioeng. Biotechnol. 7 (2019) 435.
[51] M.S. Tabatabaei, R. Islam, M. Ahmed, Applications of gold nanoparticles in ELISA, PCR, and immuno-PCR assays: a review, Anal. Chim. Acta 1143 (2021) 250–266.
[52] Y. Tsuyama, K. Mawatari, Detection and characterization of individual nanoparticles in a liquid by photothermal optical diffraction and nanofluidics, Anal. Chem. 92 (4) (2020) 3434–3439.
[53] L.E. Cole, et al., Gold nanoparticles as contrast agents in x-ray imaging and computed tomography, Nanomedicine (London) 10 (2) (2015) 321–341.
[54] C. Felton, et al., Magnetic nanoparticles as contrast agents in biomedical imaging: recent advances in iron- and manganese-based magnetic nanoparticles, Drug Metab. Rev. 46 (2) (2014) 142–154.
[55] J. Wallyn, N. Anton, T.F. Vandamme, Synthesis, principles, and properties of magnetite nanoparticles for in vivo imaging applications-a review, Pharmaceutics 11 (11) (2019).
[56] S. Sharifi, et al., Superparamagnetic iron oxide nanoparticles for in vivo molecular and cellular imaging, Contrast Media Mol. Imaging 10 (5) (2015) 329–355.
[57] I. Khalin, et al., Ultrabright fluorescent polymeric nanoparticles with a stealth Pluronic Shell for live tracking in the mouse brain, ACS Nano 14 (8) (2020) 9755–9770.
[58] X. Gao, et al., Guiding brain-tumor surgery via blood-brain-barrier-permeable gold Nanoprobes with acid-triggered MRI/SERRS signals, Adv. Mater. 29 (21) (2017).
[59] J. Debatisse, et al., PET-MRI nanoparticles imaging of blood-brain barrier damage and modulation after stroke reperfusion, Brain Commun. 2 (2) (2020) fcaa193.
[60] L. Zhao, et al., Chlorotoxin peptide-functionalized polyethylenimine-entrapped gold nanoparticles for glioma SPECT/CT imaging and radionuclide therapy, J. Nanobiotechnol. 17 (1) (2019) 30.
[61] K.E. Sapsford, et al., Functionalizing nanoparticles with biological molecules: developing chemistries that facilitate nanotechnology, Chem. Rev. 113 (3) (2013) 1904–2074.
[62] N. Melnychuk, A.S. Klymchenko, DNA-functionalized dye-loaded polymeric nanoparticles: ultrabright FRET platform for amplified detection of nucleic acids, J. Am. Chem. Soc. 140 (34) (2018) 10856–10865.
[63] U. Schröder, B.A. Sabel, Nanoparticles, a drug carrier system to pass the blood-brain barrier, permit central analgesic effects of i.v. dalargin injections, Brain Res. 710 (1) (1996) 121–124.
[64] R.N. Alyautdin, et al., Delivery of loperamide across the blood-brain barrier with polysorbate 80-coated polybutylcyanoacrylate nanoparticles, Pharm. Res. 14 (3) (1997) 325–328.
[65] U. Schroeder, P. Sommerfeld, B.A. Sabel, Efficacy of oral dalargin-loaded nanoparticle delivery across the blood–brain barrier, Peptides 19 (4) (1998) 777–780.
[66] P. Ramge, et al., Polysorbate-80 coating enhances uptake of polybutylcyanoacrylate (PBCA)-nanoparticles by human and bovine primary brain capillary endothelial cells, Eur. J. Neurosci. 12 (6) (2000) 1931–1940.
[67] L. Demeulenaere, et al., Loperamide: an open multicentre trial and double-blind cross-over comparison with placebo in patients with chronic diarrhoea, Curr. Ther. Res. Clin. Exp. 16 (1) (1974) 32–39.
[68] R.N. Upton, Cerebral uptake of drugs in humans, Clin. Exp. Pharmacol. Physiol. 34 (8) (2007) 695–701.

[69] S. Gelperina, et al., Drug delivery to the brain using surfactant-coated poly (lactide-co-glycolide) nanoparticles: influence of the formulation parameters, Eur. J. Pharm. Biopharm. 74 (2) (2010) 157–163.
[70] Y.C. Chen, et al., Effects of surface modification of PLGA-PEG-PLGA nanoparticles on loperamide delivery efficiency across the blood-brain barrier, J. Biomater. Appl. 27 (7) (2013) 909–922.
[71] Q. Yang, et al., Photoresponsive nanocapsulation of cobra neurotoxin and enhancement of its central analgesic effects under red light, Int. J. Nanomedicine 12 (2017) 3463–3470.
[72] M. Yadav, et al., Brain targeted oral delivery of doxycycline hydrochloride encapsulated tween 80 coated chitosan nanoparticles against ketamine induced psychosis: behavioral, biochemical, neurochemical and histological alterations in mice, Drug Deliv. 24 (1) (2017) 1429–1440.
[73] L. Sadeghi, V.Y. Babadi, F. Tanwir, Manganese dioxide nanoparticle induces Parkinson like neurobehavioral abnormalities in rats, Bratisl. Lek. Listy 119 (6) (2018) 379–384.
[74] L. Lugasi, et al., Proteinoid nanocapsules as drug delivery system for improving antipsychotic activity of risperidone, Molecules 25 (17) (2020).
[75] B.G. Tuna, et al., Electrophysiological effects of polyethylene glycol modified gold nanoparticles on mouse hippocampal neurons, Heliyon 6 (12) (2020) e05824.
[76] L. Lugasi, et al., Designed proteinoid polymers and nanoparticles encapsulating risperidone for enhanced antipsychotic activity, J. Nanobiotechnol. 18 (1) (2020) 149.
[77] L. Godfrey, et al., Nanoparticulate peptide delivery exclusively to the brain produces tolerance free analgesia, J. Control. Release 270 (2018) 135–144.
[78] S. Sveinbjornsdottir, The clinical symptoms of Parkinson's disease, J. Neurochem. 139 (Suppl. 1) (2016) 318–324.
[79] P. Kundu, et al., Delivery of dual drug loaded lipid based nanoparticles across the blood-brain barrier impart enhanced neuroprotection in a rotenone induced mouse model of Parkinson's disease, ACS Chem. Neurosci. 7 (12) (2016) 1658–1670.
[80] S. Hernando, et al., Intranasal administration of TAT-conjugated lipid Nanocarriers loading GDNF for Parkinson's disease, Mol. Neurobiol. 55 (1) (2018) 145–155.
[81] N. Zhang, et al., Localized delivery of curcumin into brain with polysorbate 80-modified cerasomes by ultrasound-targeted microbubble destruction for improved Parkinson's disease therapy, Theranostics 8 (8) (2018) 2264–2277.
[82] F. Jahansooz, et al., Dopamine-loaded poly (butyl cyanoacrylate) nanoparticles reverse behavioral deficits in Parkinson's animal models, Ther. Deliv. 11 (6) (2020) 387–399.
[83] Y. Liu, et al., Highly stabilized nanocrystals delivering Ginkgolide B in protecting against the Parkinson's disease, Int. J. Pharm. 577 (2020) 119053.
[84] Z. Zhang, et al., Systemic dendrimer-drug nanomedicines for long-term treatment of mild-moderate cerebral palsy in a rabbit model, J. Neuroinflammation 17 (1) (2020) 319.
[85] E. Nance, et al., Nanoscale effects in dendrimer-mediated targeting of neuroinflammation, Biomaterials 101 (2016) 96–107.
[86] A.S. Joshi, et al., Biodegradable nanoparticles containing mechanism based peptide inhibitors reduce Polyglutamine aggregation in cell models and alleviate motor symptoms in a Drosophila model of Huntington's disease, ACS Chem. Neurosci. 10 (3) (2019) 1603–1614.
[87] G. Birolini, et al., Insights into kinetics, release, and behavioral effects of brain-targeted hybrid nanoparticles for cholesterol delivery in Huntington's disease, J. Control. Release 330 (2021) 587–598.
[88] D. Sun, et al., Design of PLGA-functionalized quercetin nanoparticles for potential use in Alzheimer's disease, Colloids Surf. B: Biointerfaces 148 (2016) 116–129.
[89] Y. Liu, et al., Microbubbles in combination with focused ultrasound for the delivery of quercetin-modified sulfur nanoparticles through the blood brain barrier into the brain parenchyma and relief of endoplasmic reticulum stress to treat Alzheimer's disease, Nanoscale 12 (11) (2020) 6498–6511.
[90] N. Rishitha, A. Muthuraman, Therapeutic evaluation of solid lipid nanoparticle of quercetin in pentylenetetrazole induced cognitive impairment of zebrafish, Life Sci. 199 (2018) 80–87.
[91] A.K. Singh, et al., Lipid-coated MCM-41 mesoporous silica nanoparticles loaded with Berberine improved inhibition of acetylcholine esterase and amyloid formation, ACS Biomater Sci. Eng. 7 (8) (2021) 3737–3753.
[92] T. Dara, et al., Improvement of memory deficits in the rat model of Alzheimer's disease by erythropoietin-loaded solid lipid nanoparticles, Neurobiol. Learn. Mem. 166 (2019) 107082.
[93] Q. Guo, et al., A dual-ligand fusion peptide improves the brain-neuron targeting of nanocarriers in Alzheimer's disease mice, J. Control. Release 320 (2020) 347–362.
[94] E. Sanchez-Lopez, et al., Memantine loaded PLGA PEGylated nanoparticles for Alzheimer's disease: in vitro and in vivo characterization, J. Nanobiotechnol. 16 (1) (2018) 32.
[95] P.V. Kulkarni, et al., Quinoline-n-butylcyanoacrylate-based nanoparticles for brain targeting for the diagnosis of Alzheimer's disease, Wiley Interdiscip. Rev. Nanomed. Nanobiotechnol. 2 (1) (2010) 35–47.
[96] M. Silva-Abreu, et al., PPARgamma agonist-loaded PLGA-PEG nanocarriers as a potential treatment for Alzheimer's disease: in vitro and in vivo studies, Int. J. Nanomedicine 13 (2018) 5577–5590.
[97] A.R. Bilia, et al., Successful brain delivery of andrographolide loaded in human albumin nanoparticles to TgCRND8 mice, an Alzheimer's disease mouse model, Front. Pharmacol. 10 (2019) 910.
[98] S.K. Verma, et al., Enhancement in the neuroprotective power of Riluzole against cerebral ischemia using a brain targeted drug delivery vehicle, ACS Appl. Mater. Interfaces 8 (30) (2016) 19716–19723.
[99] W.B. Hubbard, et al., Hemostatic nanoparticles increase survival, mitigate neuropathology and alleviate anxiety in a rodent blast trauma model, Sci. Rep. 8 (1) (2018) 10622.
[100] H.J. Byeon, et al., Doxorubicin-loaded nanoparticles consisted of cationic- and mannose-modified-albumins for dual-targeting in brain tumors, J. Control. Release 225 (2016) 301–313.
[101] X. Xu, et al., A novel doxorubicin loaded folic acid conjugated PAMAM modified with borneol, a nature dual-functional product of reducing PAMAM toxicity and boosting BBB penetration, Eur. J. Pharm. Sci. 88 (2016) 178–190.
[102] Y. Zhang, et al., Enhanced anti-tumor effects of doxorubicin on glioma by entrapping in polybutylcyanoacrylate nanoparticles, Tumour Biol. 37 (2) (2016) 2703–2708.
[103] W. Niu, et al., A biomimetic drug delivery system by integrating grapefruit extracellular vesicles and doxorubicin-loaded heparin-based nanoparticles for glioma therapy, Nano Lett. 21 (3) (2021) 1484–1492.
[104] X. Shi, et al., iRGD and TGN co-modified PAMAM for multi-targeted delivery of ATO to gliomas, Biochem. Biophys. Res. Commun. 527 (1) (2020) 117–123.
[105] M. Yu, et al., D-T7 peptide-modified PEGylated bilirubin nanoparticles loaded with Cediranib and paclitaxel for Antiangiogenesis and chemotherapy of glioma, ACS Appl. Mater. Interfaces 11 (1) (2019) 176–186.
[106] S.J. Smith, et al., Overall survival in malignant glioma is significantly prolonged by neurosurgical delivery of etoposide and Temozolomide from a Thermo-responsive biodegradable paste, Clin. Cancer Res. 25 (16) (2019) 5094–5106.
[107] J. Guan, et al., Cholera toxin subunit b enabled multifunctional glioma-targeted drug delivery, Adv. Healthc. Mater. 6 (23) (2017).
[108] G. Wang, et al., Quercetin-loaded freeze-dried nanomicelles: improving absorption and anti-glioma efficiency in vitro and in vivo, J. Control. Release 235 (2016) 276–290.
[109] Y.E. Seo, et al., Nanoparticle-mediated intratumoral inhibition of miR-21 for improved survival in glioblastoma, Biomaterials 201 (2019) 87–98.
[110] J.V. Gregory, et al., Systemic brain tumor delivery of synthetic protein nanoparticles for glioblastoma therapy, Nat. Commun. 11 (1) (2020) 5687.
[111] Q. Yang, et al., Gene therapy for drug-resistant glioblastoma via lipid-polymer hybrid nanoparticles combined with focused ultrasound, Int. J. Nanomedicine 16 (2021) 185–199.
[112] X. Ju, et al., Prodrug delivery using dual-targeting nanoparticles to treat breast Cancer brain metastases, Mol. Pharm. 18 (7) (2021) 2694–2702.
[113] D. Gonzalez-Carter, et al., Quantification of blood-brain barrier transport and neuronal toxicity of unlabelled multiwalled carbon nanotubes as a function of surface charge, Nanoscale 11 (45) (2019) 22054–22069.
[114] A.N. Ananth, et al., PVA and BSA stabilized silver nanoparticles based surface-enhanced plasmon resonance probes for protein detection, Colloids Surf. B: Biointerfaces 85 (2) (2011) 138–144.
[115] C. Chen, et al., Imaging of neurotransmitters and small molecules in brain tissues using laser desorption/ionization mass spectrometry assisted with zinc oxide nanoparticles, J. Am. Soc. Mass Spectrom. 32 (4) (2021) 1065–1079.
[116] P. Arranz-Gibert, et al., A MALDI-TOF-based method for studying the transport of BBB shuttles-enhancing sensitivity and versatility of cell-based in vitro transport models, Sci. Rep. 9 (1) (2019) 4875.
[117] H.R. Kim, et al., Analysis of plasma protein adsorption onto PEGylated nanoparticles by complementary methods: 2-DE, CE and Protein Lab-on-chip system, Electrophoresis 28 (13) (2007) 2252–2261.
[118] I.L. Hsiao, et al., Quantification and visualization of cellular uptake of TiO2 and ag nanoparticles: comparison of different ICP-MS techniques, J. Nanobiotechnol. 14 (1) (2016) 50.
[119] R. Bai, et al., Integrated analytical techniques with high sensitivity for studying brain translocation and potential impairment induced by intranasally instilled copper nanoparticles, Toxicol. Lett. 226 (1) (2014) 70–80.
[120] B.L. Milman, General principles of identification by mass spectrometry, TrAC Trends Anal. Chem. 69 (2015) 24–33.
[121] Y. Zhang, L. Liu, L. Ren, Liquid chromatography-tandem mass spectrometry (LC-MS/MS) determination of cantharidin in biological specimens and application to postmortem interval estimation in cantharidin poisoning, Sci. Rep. 10 (1) (2020) 10438.
[122] X. Li, et al., Odorranalectin modified PEG-PLGA/PEG-PBLG curcumin-loaded nanoparticle for intranasal administration, Drug Dev. Ind. Pharm. 46 (6) (2020) 899–909.
[123] P. Girotra, S.K. Singh, G. Kumar, Development of zolmitriptan loaded PLGA/poloxamer nanoparticles for migraine using quality by design approach, Int. J. Biol. Macromol. 85 (2016) 92–101.
[124] T.N. Pashirova, et al., Nanoparticle-delivered 2-PAM for rat brain protection against paraoxon central toxicity, ACS Appl. Mater. Interfaces 9 (20) (2017) 16922–16932.
[125] H. Li, et al., Lactoferrin functionalized PEG-PLGA nanoparticles of shikonin for brain targeting therapy of glioma, Int. J. Biol. Macromol. 107 (Pt A) (2018) 204–211.
[126] T.K. Shaw, et al., Successful delivery of docetaxel to rat brain using experimentally developed nanoliposome: a treatment strategy for brain tumor, Drug Deliv. 24 (1) (2017) 346–357.
[127] L. Dutta, et al., Lipid-based nanocarrier efficiently delivers highly water soluble drug across the blood-brain barrier into brain, Drug Deliv. 25 (1) (2018) 504–516.

[128] S. Liu, S. Yang, P.C. Ho, Intranasal administration of carbamazepine-loaded carboxymethyl chitosan nanoparticles for drug delivery to the brain, Asian J. Pharm. Sci. 13 (1) (2018) 72–81.
[129] Y. Jiang, et al., The optimization design of lactoferrin loaded HupA nanoemulsion for targeted drug transport via intranasal route, Int. J. Nanomedicine 14 (2019) 9217–9234.
[130] Y. Gong, et al., An Elvitegravir nanoformulation crosses the blood-brain barrier and suppresses HIV-1 replication in microglia, Viruses 12 (5) (2020).
[131] R.R. Kudarha, K.K. Sawant, Chondroitin sulfate conjugation facilitates tumor cell internalization of albumin nanoparticles for brain-targeted delivery of temozolomide via CD44 receptor-mediated targeting, Drug Deliv. Transl. Res. 11 (5) (2021) 1994–2008.
[132] B. Wilson, et al., Albumin nanoparticles coated with polysorbate 80 for the targeted delivery of antiepileptic drug levetiracetam into the brain, Drug Deliv. Transl. Res. 10 (6) (2020) 1853–1861.
[133] I. Singh, et al., Lactoferrin bioconjugated solid lipid nanoparticles: a new drug delivery system for potential brain targeting, J. Drug Target. 24 (3) (2016) 212–223.
[134] C. Lei, et al., Development of nanoparticles for drug delivery to brain tumor: the effect of surface materials on penetration into brain tissue, J. Pharm. Sci. 108 (5) (2019) 1736–1745.
[135] A. Cano, et al., Dual-drug loaded nanoparticles of Epigallocatechin-3-gallate (EGCG)/ascorbic acid enhance therapeutic efficacy of EGCG in a APPswe/PS1dE9 Alzheimer's disease mice model, J. Control. Release 301 (2019) 62–75.
[136] E. Marin, et al., New curcumin-loaded chitosan nanocapsules: in vivo evaluation, Planta Med. 83 (10) (2017) 877–883.
[137] P. Kumar, et al., Stearic acid based, systematically designed oral lipid nanoparticles for enhanced brain delivery of dimethyl fumarate, Nanomedicine (London) 12 (23) (2017) 2607–2621.
[138] X. Wan, et al., Lapatinib-loaded human serum albumin nanoparticles for the prevention and treatment of triple-negative breast cancer metastasis to the brain, Oncotarget 7 (23) (2016) 34038–34051.
[139] S.H. Omar, et al., Bioinspired lipid-polysaccharide modified hybrid nanoparticles as a brain-targeted highly loaded carrier for a hydrophilic drug, Int. J. Biol. Macromol. 165 (Pt A) (2020) 483–494.
[140] H. He, et al., Solid lipid nanoparticles as a drug delivery system to across the blood-brain barrier, Biochem. Biophys. Res. Commun. 519 (2) (2019) 385–390.
[141] Z. Karami, et al., Magnetic brain targeting of naproxen-loaded polymeric micelles: pharmacokinetics and biodistribution study, Mater. Sci. Eng. C Mater. Biol. Appl. 100 (2019) 771–780.
[142] B. Ji, et al., Combining nanoscale magnetic nimodipine liposomes with magnetic resonance image for Parkinson's disease targeting therapy, Nanomedicine (London) 12 (3) (2017) 237–253.
[143] R.A.H. Ishak, N.M. Mostafa, A.O. Kamel, Stealth lipid polymer hybrid nanoparticles loaded with rutin for effective brain delivery - comparative study with the gold standard (tween 80): optimization, characterization and biodistribution, Drug Deliv. 24 (1) (2017) 1874–1890.
[144] L. Yang, et al., Development a hyaluronic acid ion-pairing liposomal nanoparticle for enhancing anti-glioma efficacy by modulating glioma microenvironment, Drug Deliv. 25 (1) (2018) 388–397.
[145] A. Gothwal, et al., Boosted memory and improved brain bioavailability of Rivastigmine: targeting effort to the brain using covalently tethered lower generation PAMAM dendrimers with Lactoferrin, Mol. Pharm. 15 (10) (2018) 4538–4549.
[146] S. Lahkar, M. Kumar Das, Surface modified kokum butter lipid nanoparticles for the brain targeted delivery of nevirapine, J. Microencapsul. 35 (7–8) (2018) 680–694.
[147] K.B. Johnsen, et al., Antibody affinity and valency impact brain uptake of transferrin receptor-targeted gold nanoparticles, Theranostics 8 (12) (2018) 3416–3436.
[148] S. Ohta, et al., Investigating the optimum size of nanoparticles for their delivery into the brain assisted by focused ultrasound-induced blood-brain barrier opening, Sci. Rep. 10 (1) (2020) 18220.
[149] C. Ugur Yilmaz, et al., Targeted delivery of lacosamide-conjugated gold nanoparticles into the brain in temporal lobe epilepsy in rats, Life Sci. 257 (2020) 118081.
[150] B. Su, et al., Effect of retro-Inverso isomer of bradykinin on size-dependent penetration of blood-brain tumor barrier, Small 14 (7) (2018).
[151] R. Enteshari Najafabadi, et al., Using superparamagnetic iron oxide nanoparticles to enhance bioavailability of quercetin in the intact rat brain, BMC Pharmacol. Toxicol. 19 (1) (2018) 59.
[152] J.C. Mamo, et al., Sodium alginate capsulation increased brain delivery of probucol and suppressed neuroinflammation and neurodegeneration, Ther. Deliv. 9 (10) (2018) 703–709.
[153] M. Yemisci, et al., Preparation and characterization of biocompatible chitosan nanoparticles for targeted brain delivery of peptides, Methods Mol. Biol. 1727 (2018) 443–454.
[154] D. Coluccia, et al., Enhancing glioblastoma treatment using cisplatin-gold-nanoparticle conjugates and targeted delivery with magnetic resonance-guided focused ultrasound, Nanomedicine 14 (4) (2018) 1137–1148.
[155] R.G. Madane, H.S. Mahajan, Curcumin-loaded nanostructured lipid carriers (NLCs) for nasal administration: design, characterization, and in vivo study, Drug Deliv. 23 (4) (2016) 1326–1334.
[156] Sonali, et al., Transferrin liposomes of docetaxel for brain-targeted cancer applications: formulation and brain theranostics, Drug Deliv. 23 (4) (2016) 1261–1271.
[157] J. Shen, et al., Ginsenoside Rg1 nanoparticle penetrating the blood-brain barrier to improve the cerebral function of diabetic rats complicated with cerebral infarction, Int. J. Nanomedicine 12 (2017) 6477–6486.
[158] L. Kou, et al., L-carnitine-conjugated nanoparticles to promote permeation across blood-brain barrier and to target glioma cells for drug delivery via the novel organic cation/carnitine transporter OCTN2, Artif. Cells Nanomed. Biotechnol. 46 (8) (2018) 1605–1616.
[159] B.O. Yuan, et al., Cell-penetrating peptide-coated liposomes for drug delivery across the blood-brain barrier, Anticancer Res. 39 (1) (2019) 237–243.
[160] A. Mukherjee, et al., Neuro-protective role of nanocapsulated curcumin against cerebral ischemia-reperfusion induced oxidative injury, Brain Res. 1704 (2019) 164–173.
[161] Q. Bao, et al., Simultaneous blood-brain barrier crossing and protection for stroke treatment based on Edaravone-loaded ceria nanoparticles, ACS Nano 12 (7) (2018) 6794–6805.
[162] B. Wilson, et al., Poly(n-butylcyanoacrylate) nanoparticles coated with polysorbate 80 for the targeted delivery of rivastigmine into the brain to treat Alzheimer's disease, Brain Res. 1200 (2008) 159–168.
[163] N.M. Harris, et al., Nano-particle delivery of brain derived neurotrophic factor after focal cerebral ischemia reduces tissue injury and enhances behavioral recovery, Pharmacol. Biochem. Behav. 150-151 (2016) 48–56.
[164] X.Y. Meng, et al., Vascular endothelial growth factor-loaded poly-lactic-co-glycolic acid nanoparticles with controlled release protect the dopaminergic neurons in Parkinson's rats, Chem. Biol. Drug Des. 95 (6) (2020) 631–639.
[165] F. Sousa, et al., Enhanced anti-angiogenic effects of bevacizumab in glioblastoma treatment upon intranasal administration in polymeric nanoparticles, J. Control. Release 309 (2019) 37–47.
[166] Y.Z. Zhao, et al., Intranasal delivery of bFGF with nanoliposomes enhances in vivo neuroprotection and neural injury recovery in a rodent stroke model, J. Control. Release 224 (2016) 165–175.
[167] C. Shen, Z. Zhang, An overview of nanoparticle-assisted polymerase chain reaction technology, In Bio-Nanotechnol. (2013) 97–106.
[168] P. Fan, et al., Enhanced sensitivity for detection of HIV-1 p24 antigen by a novel nuclease-linked fluorescence oligonucleotide assay, PLoS One 10 (4) (2015) e0125701.
[169] L. Chen, et al., Gold nanoparticle enhanced immuno-PCR for ultrasensitive detection of Hantaan virus nucleocapsid protein, J. Immunol. Methods 346 (1–2) (2009) 64–70.
[170] F. Shabanpoor, et al., Identification of a peptide for systemic brain delivery of a Morpholino oligonucleotide in mouse models of spinal muscular atrophy, Nucleic Acid Ther. 27 (3) (2017) 130–143.
[171] P. Ramalingam, et al., Lipid nanoparticles improve the uptake of alpha-Asarone into the brain parenchyma: formulation, characterization, in vivo pharmacokinetics, and brain delivery, AAPS PharmSciTech 21 (8) (2020) 299.
[172] J. Liu, et al., Functionalized nanocarrier combined seizure-specific vector with P-glycoprotein modulation property for antiepileptic drug delivery, Biomaterials 74 (2016) 64–76.
[173] H. Wei, et al., A novel delivery method of cyclovirobuxine D for brain-targeting: chitosan coated nanoparticles loading cyclovirobuxine D by intranasal administration, J. Nanosci. Nanotechnol. 18 (8) (2018) 5274–5282.
[174] Y. Wang, et al., Protecting neurons from cerebral ischemia/reperfusion injury via nanoparticle-mediated delivery of an siRNA to inhibit microglial neurotoxicity, Biomaterials 161 (2018) 95–105.
[175] P. Yin, et al., Intranasal delivery of immunotherapeutic nanoformulations for treatment of glioma through in situ activation of immune response, Int. J. Nanomedicine 15 (2020) 1499–1515.
[176] B. Surnar, et al., Nanotechnology-mediated crossing of two impermeable membranes to modulate the stars of the neurovascular unit for neuroprotection, Proc. Natl. Acad. Sci. USA 115 (52) (2018) E12333–E12342.
[177] E. Sulheim, et al., Therapeutic effect of Cabazitaxel and blood-brain barrier opening in a patient-derived glioblastoma model, Nanotheranostics 3 (1) (2019) 103–112.
[178] A. Parmar, et al., Anti-proliferate and apoptosis triggering potential of methotrexate-transferrin conjugate encapsulated PLGA nanoparticles with enhanced cellular uptake by high-affinity folate receptors, Artif. Cells Nanomed. Biotechnol. 46 (sup2) (2018) 704–719.
[179] S. Kumari, et al., Overcoming blood brain barrier with a dual purpose Temozolomide loaded Lactoferrin nanoparticles for combating glioma (SERP-17-12433), Sci. Rep. 7 (1) (2017) 6602.
[180] C.H. Fan, et al., Enhancing boron uptake in brain glioma by a boron-polymer/microbubble complex with focused ultrasound, ACS Appl. Mater. Interfaces 11 (12) (2019) 11144–11156.
[181] G.H. Bode, et al., An in vitro and in vivo study of peptide-functionalized nanoparticles for brain targeting: the importance of selective blood-brain barrier uptake, Nanomedicine 13 (3) (2017) 1289–1300.
[182] E.A. Wyatt, M.E. Davis, Method of establishing breast cancer brain metastases affects brain uptake and efficacy of targeted, therapeutic nanoparticles, Bioeng. Transl. Med. 4 (1) (2019) 30–37.
[183] A. Sharma, et al., Effect of mannose targeting of hydroxyl PAMAM dendrimers on cellular and organ biodistribution in a neonatal brain injury model, J. Control. Release 283 (2018) 175–189.
[184] R. Gromnicova, et al., Localization and mobility of glucose-coated gold nanoparticles within the brain, Nanomedicine (London) 11 (6) (2016) 617–625.
[185] M. Kumar, et al., Nanoparticle biodistribution coefficients: a quantitative approach for understanding the tissue distribution of nanoparticles, Adv. Drug Deliv. Rev. 194 (2023) 114708.

[186] S. Kumar, et al., Selegiline Nanoformulation in attenuation of oxidative stress and upregulation of dopamine in the brain for the treatment of Parkinson's disease, Rejuvenation Res. 21 (5) (2018) 464–476.
[187] S. Gupta, et al., Systematic approach for the formulation and optimization of solid lipid nanoparticles of Efavirenz by high pressure homogenization using design of experiments for brain targeting and enhanced bioavailability, Biomed. Res. Int. 2017 (2017) 5984014.
[188] S. Paris-Robidas, et al., Internalization of targeted quantum dots by brain capillary endothelial cells in vivo, J. Cereb. Blood Flow Metab. 36 (4) (2016) 731–742.
[189] Z. Karami, et al., Neuropharmacokinetic evaluation of lactoferrin-treated indinavir-loaded nanoemulsions: remarkable brain delivery enhancement, Drug Dev. Ind. Pharm. 45 (5) (2019) 736–744.
[190] B. Shah, et al., Application of box-Behnken design for optimization and development of quetiapine fumarate loaded chitosan nanoparticles for brain delivery via intranasal route*, Int. J. Biol. Macromol. 89 (2016) 206–218.
[191] S.A. Kumbhar, et al., Preparation, characterization, and optimization of asenapine maleate mucoadhesive nanoemulsion using box-Behnken design: in vitro and in vivo studies for brain targeting, Int. J. Pharm. 586 (2020) 119499.
[192] S.K. Bhattamisra, et al., Nose to brain delivery of rotigotine loaded chitosan nanoparticles in human SH-SY5Y neuroblastoma cells and animal model of Parkinson's disease, Int. J. Pharm. 579 (2020) 119148.
[193] H. Chen, et al., Focused ultrasound-enhanced intranasal brain delivery of brain-derived neurotrophic factor, Sci. Rep. 6 (2016) 28599.
[194] E. Ahmad, et al., Evidence of nose-to-brain delivery of nanoemulsions: cargoes but not vehicles, Nanoscale 9 (3) (2017) 1174–1183.
[195] N. Shrestha, et al., Tailoring midazolam-loaded chitosan nanoparticulate formulation for enhanced brain delivery via intranasal route, Polymers (Basel) 12 (11) (2020).
[196] R.J. Patel, R.H. Parikh, Intranasal delivery of topiramate nanoemulsion: pharmacodynamic, pharmacokinetic and brain uptake studies, Int. J. Pharm. 585 (2020) 119486.
[197] S.R. Pailla, et al., Intranasal Zotepine nanosuspension: intended for improved brain distribution in rats, Daru 27 (2) (2019) 541–556.
[198] G.M. Jojo, et al., Formulation and optimization of intranasal nanolipid carriers of pioglitazone for the repurposing in Alzheimer's disease using box-Behnken design, Drug Dev. Ind. Pharm. 45 (7) (2019) 1061–1072.
[199] A. Hefnawy, I.A. Khalil, I.M. El-Sherbiny, Facile development of nanocomplex-in-nanoparticles for enhanced loading and selective delivery of doxorubicin to brain, Nanomedicine (London) 12 (24) (2017) 2737–2761.
[200] A.M. Fatouh, A.H. Elshafeey, A. Abdelbary, Intranasal agomelatine solid lipid nanoparticles to enhance brain delivery: formulation, optimization and in vivo pharmacokinetics, Drug Des. Devel. Ther. 11 (2017) 1815–1825.
[201] N. Ahmad, et al., Quantification and brain targeting of eugenol-loaded surface modified nanoparticles through intranasal route in the treatment of cerebral ischemia, Drug. Res. (Stuttg) 68 (10) (2018) 584–595.
[202] R. Li, et al., Targeted delivery of intranasally administered nanoparticles-mediated neuroprotective peptide NR2B9c to brain and neuron for treatment of ischemic stroke, Nanomedicine 18 (2019) 380–390.
[203] A. Shobo, et al., Enhanced brain penetration of pretomanid by intranasal administration of an oil-in-water nanoemulsion, Nanomedicine (London) 13 (9) (2018) 997–1008.
[204] D. Maussang, et al., Glutathione conjugation dose-dependently increases brain-specific liposomal drug delivery in vitro and in vivo, Drug Discov. Today Technol. 20 (2016) 59–69.
[205] J. Tao, et al., Angiopep-2-conjugated "Core-Shell" hybrid nanovehicles for targeted and pH-triggered delivery of arsenic trioxide into glioma, Mol. Pharm. 16 (2) (2019) 786–797.
[206] J. Zhu, et al., Intranasal administration of pullulan-based nanoparticles for enhanced delivery of adriamycin into the brain: in vitro and in vivo evaluation, Pharmazie 74 (1) (2019) 39–46.
[207] V.I. Chefer, et al., Overview of brain microdialysis, Curr. Protoc. Neurosci. Chapter 7 (2009) p. Unit7 1.
[208] M. Zhao, et al., Nanocarrier-based drug combination therapy for glioblastoma, Theranostics 10 (3) (2020) 1355–1372.
[209] T. Schuster, et al., Potential of surfactant-coated nanoparticles to improve brain delivery of arylsulfatase a, J. Control. Release 253 (2017) 1–10.
[210] J.E. Dahlman, et al., Barcoded nanoparticles for high throughput in vivo discovery of targeted therapeutics, Proc. Natl. Acad. Sci. USA 114 (8) (2017) 2060–2065.
[211] T. Feczko, et al., Stimulating brain recovery after stroke using theranostic albumin nanocarriers loaded with nerve growth factor in combination therapy, J. Control. Release 293 (2019) 63–72.
[212] V.N. Bharadwaj, et al., Sex-dependent macromolecule and nanoparticle delivery in experimental brain injury, Tissue Eng. Part A 26 (13–14) (2020) 688–701.
[213] Y.Z. Zhao, et al., Glioma-targeted therapy using Cilengitide nanoparticles combined with UTMD enhanced delivery, J. Control. Release 224 (2016) 112–125.
[214] M. Orunoglu, et al., Effects of curcumin-loaded PLGA nanoparticles on the RG2 rat glioma model, Mater. Sci. Eng. C Mater. Biol. Appl. 78 (2017) 32–38.
[215] C. He, et al., LRP1-mediated pH-sensitive polymersomes facilitate combination therapy of glioblastoma in vitro and in vivo, J. Nanobiotechnol. 19 (1) (2021) 29.
[216] H. Baghirov, et al., Ultrasound-mediated delivery and distribution of polymeric nanoparticles in the normal brain parenchyma of a metastatic brain tumour model, PLoS One 13 (1) (2018) e0191102.
[217] J.S. Young, et al., Convection-enhanced delivery of polymeric nanoparticles encapsulating chemotherapy in canines with spontaneous supratentorial tumors, World Neurosurg. 117 (2018) e698–e704.
[218] H.A. Miller, et al., Evaluating differential nanoparticle accumulation and retention kinetics in a mouse model of traumatic brain injury via K(trans) mapping with MRI, Sci. Rep. 9 (1) (2019) 16099.
[219] A. Conti, et al., Empirical and theoretical characterization of the diffusion process of different gadolinium-based nanoparticles within the brain tissue after ultrasound-induced permeabilization of the blood-brain barrier, Contrast Media Mol. Imaging 2019 (2019) 6341545.
[220] C. Corot, et al., Recent advances in iron oxide nanocrystal technology for medical imaging, Adv. Drug Deliv. Rev. 58 (14) (2006) 1471–1504.
[221] J.W. Bulte, D.L. Kraitchman, Iron oxide MR contrast agents for molecular and cellular imaging, NMR Biomed. 17 (7) (2004) 484–499.
[222] M.R. Mohammadi, et al., PEG/dextran double layer influences Fe ion release and colloidal stability of Iron oxide nanoparticles, Sci. Rep. 8 (1) (2018) 4286.
[223] C.C. Hanot, et al., Effects of Iron-oxide nanoparticle surface chemistry on uptake kinetics and cytotoxicity in CHO-K1 cells, Int. J. Mol. Sci. 17 (1) (2015).
[224] J.H. Fang, et al., Dual-targeting Lactoferrin-conjugated polymerized magnetic Polydiacetylene-assembled Nanocarriers with self-responsive fluorescence/magnetic resonance imaging for in vivo brain tumor therapy, Adv. Healthc. Mater. 5 (6) (2016) 688–695.
[225] G. Jia, et al., NRP-1 targeted and cargo-loaded exosomes facilitate simultaneous imaging and therapy of glioma in vitro and in vivo, Biomaterials 178 (2018) 302–316.
[226] Y. Wang, et al., The treatment value of IL-1beta monoclonal antibody under the targeting location of alpha-methyl-L-tryptophan and superparamagnetic iron oxide nanoparticles in an acute temporal lobe epilepsy model, J. Transl. Med. 16 (1) (2018) 337.
[227] M. Gauberti, et al., Molecular Magnetic Resonance Imaging of Brain–Immune Interactions, 2014.
[228] T.H. Shin, et al., High-resolution T1 MRI via renally clearable dextran nanoparticles with an iron oxide shell, Nat. Biomed. Eng. 5 (3) (2021) 252–263.
[229] M.A. McAteer, et al., In vivo magnetic resonance imaging of acute brain inflammation using microparticles of iron oxide, Nat. Med. 13 (10) (2007) 1253–1258.
[230] M. Gauberti, et al., Molecular magnetic resonance imaging of endothelial activation in the central nervous system, Theranostics 8 (5) (2018) 1195–1212.
[231] M. Gauberti, et al., Ultra-sensitive molecular MRI of vascular cell adhesion molecule-1 reveals a dynamic inflammatory penumbra after strokes, Stroke 44 (7) (2013) 1988–1996.
[232] A. Quenault, et al., Molecular magnetic resonance imaging discloses endothelial activation after transient ischaemic attack, Brain 140 (1) (2017) 146–157.
[233] A. Montagne, et al., Ultra-sensitive molecular MRI of cerebrovascular cell activation enables early detection of chronic central nervous system disorders, Neuroimage 63 (2) (2012) 760–770.
[234] S. Serres, et al., VCAM-1-targeted magnetic resonance imaging reveals subclinical disease in a mouse model of multiple sclerosis, FASEB J. 25 (12) (2011) 4415–4422.
[235] Y. Zhu, et al., Magnetic resonance imaging of radiation-induced brain injury using targeted microparticles of iron oxide, Acta Radiol. 53 (7) (2012) 812–819.
[236] S. de Lizarrondo Martinez, et al., Tracking the immune response by MRI using biodegradable and ultrasensitive microprobes, Sci. Adv. 8 (28) (2022) p. eabm3596-eabm3596.
[237] J. Estelrich, M.J. Sanchez-Martin, M.A. Busquets, Nanoparticles in magnetic resonance imaging: from simple to dual contrast agents, Int. J. Nanomedicine 10 (2015) 1727–1741.
[238] L. Marti-Bonmati, et al., Multimodality imaging techniques, Contrast Media Mol. Imaging 5 (4) (2010) 180–189.
[239] M. Lecchi, et al., Current concepts on imaging in radiotherapy, Eur. J. Nucl. Med. Mol. Imaging 35 (4) (2008) 821–837.
[240] R. Juthani, et al., Ultrasmall Core-Shell silica nanoparticles for precision drug delivery in a high-grade malignant brain tumor model, Clin. Cancer Res. 26 (1) (2020) 147–158.
[241] C.W. Huang, et al., Integrin alpha2beta1-targeting ferritin nanocarrier traverses the blood-brain barrier for effective glioma chemotherapy, J. Nanobiotechnol. 19 (1) (2021) 180.
[242] Y. Cui, et al., Dual-targeting magnetic PLGA nanoparticles for codelivery of paclitaxel and curcumin for brain tumor therapy, ACS Appl. Mater. Interfaces 8 (47) (2016) 32159–32169.
[243] S. Gonawala, M.M. Ali, Application of dendrimer-based nanoparticles in glioma imaging, J. Nanomed. Nanotechnol. 8 (3) (2017).
[244] Y. Chen, et al., Efficient cholera toxin B subunit-based nanoparticles with MRI capability for drug delivery to the brain following intranasal administration, Macromol. Biosci. 19 (2) (2019) e1800340.
[245] X. Liu, et al., Engineered superparamagnetic iron oxide nanoparticles (SPIONs) for dual-modality imaging of intracranial glioblastoma via EGFRvIII targeting, Beilstein J. Nanotechnol. 10 (2019) 1860–1872.
[246] U.K. Sukumar, et al., Intranasal delivery of targeted polyfunctional gold-iron oxide nanoparticles loaded with therapeutic microRNAs for combined theranostic multimodality imaging and presensitization of glioblastoma to temozolomide, Biomaterials 218 (2019) 119342.
[247] B.P. Mead, et al., Focused ultrasound preconditioning for augmented nanoparticle penetration and efficacy in the central nervous system, Small 15 (49) (2019) e1903460.

[248] L. Long, et al., Treatment of Parkinson's disease in rats by Nrf2 transfection using MRI-guided focused ultrasound delivery of nanomicrobubbles, Biochem. Biophys. Res. Commun. 482 (1) (2017) 75–80.
[249] K.F. Timbie, et al., MR image-guided delivery of cisplatin-loaded brain-penetrating nanoparticles to invasive glioma with focused ultrasound, J. Control. Release 263 (2017) 120–131.
[250] V. Koo, P.W. Hamilton, K. Williamson, Non-invasive in vivo imaging in small animal research, Cell. Oncol. 28 (4) (2006) 127–139.
[251] A. Gust, et al., A starting point for fluorescence-based single-molecule measurements in biomolecular research, Molecules 19 (10) (2014) 15824–15865.
[252] J.W. Taraska, W.N. Zagotta, Fluorescence applications in molecular neurobiology, Neuron 66 (2) (2010) 170–189.
[253] D. Bousmail, et al., Precision spherical nucleic acids for delivery of anticancer drugs, Chem. Sci. 8 (9) (2017) 6218–6229.
[254] S. Sathya, et al., Phytol loaded PLGA nanoparticles ameliorate scopolamine-induced cognitive dysfunction by attenuating cholinesterase activity, oxidative stress and apoptosis in Wistar rat, Nutr. Neurosci. (2020) 1–17.
[255] H. Liu, et al., Amphiphilic Endomorphin-1 derivative functions as self-assembling nanomedicine for effective brain delivery, Chem. Pharm. Bull. (Tokyo) 67 (9) (2019) 977–984.
[256] R. Xu, et al., Rhynchophylline loaded-mPEG-PLGA nanoparticles coated with Tween-80 for preliminary study in Alzheimer's disease, Int. J. Nanomedicine 15 (2020) 1149–1160.
[257] I. Schlachet, H. Moshe Halamish, A. Sosnik, Mixed amphiphilic polymeric nanoparticles of chitosan, poly(vinyl alcohol) and poly(methyl methacrylate) for intranasal drug delivery: a preliminary in vivo study, Molecules 25 (19) (2020).
[258] C. Gao, et al., T807-modified human serum albumin biomimetic nanoparticles for targeted drug delivery across the blood-brain barrier, J. Drug Target. 28 (10) (2020) 1085–1095.
[259] R. Dal Magro, et al., ApoE-modified solid lipid nanoparticles: a feasible strategy to cross the blood-brain barrier, J. Control. Release 249 (2017) 103–110.
[260] W. Gao, et al., Rapid and efficient crossing blood-brain barrier: hydrophobic drug delivery system based on propionylated amylose helix nanoclusters, Biomaterials 113 (2017) 133–144.
[261] Y. Du, et al., Facile marriage of Gd(3+) to polymer-coated carbon nanodots with enhanced biocompatibility for targeted MR/fluorescence imaging of glioma, Int. J. Pharm. 552 (1–2) (2018) 84–90.
[262] R. Dal Magro, et al., Artificial apolipoprotein corona enables nanoparticle brain targeting, Nanomedicine 14 (2) (2018) 429–438.
[263] H. Song, et al., Enhanced permeability of blood-brain barrier and targeting function of brain via borneol-modified chemically solid lipid nanoparticle, Int. J. Nanomedicine 13 (2018) 1869–1879.
[264] M. Khongkow, et al., Surface modification of gold nanoparticles with neuron-targeted exosome for enhanced blood-brain barrier penetration, Sci. Rep. 9 (1) (2019) 8278.
[265] L.P. Wu, et al., Crossing the blood-brain-barrier with nanoligand drug carriers self-assembled from a phage display peptide, Nat. Commun. 10 (1) (2019) 4635.
[266] S. Xiong, et al., Brain-targeted delivery shuttled by black phosphorus nanostructure to treat Parkinson's disease, Biomaterials 260 (2020) 120339.
[267] B. Dos Santos Rodrigues, et al., Dual-modified liposome for targeted and enhanced gene delivery into mice brain, J. Pharmacol. Exp. Ther. 374 (3) (2020) 354–365.
[268] L. Wei, et al., Brain tumor-targeted therapy by systemic delivery of siRNA with transferrin receptor-mediated core-shell nanoparticles, Int. J. Pharm. 510 (1) (2016) 394–405.
[269] Y. Jiang, et al., Enhanced Antiglioma efficacy of ultrahigh loading capacity paclitaxel prodrug conjugate self-assembled targeted nanoparticles, ACS Appl. Mater. Interfaces 9 (1) (2017) 211–217.
[270] J. Shi, et al., An MSN-PEG-IP drug delivery system and IL13Ralpha2 as targeted therapy for glioma, Nanoscale 9 (26) (2017) 8970–8981.
[271] C. Chen, et al., Peptide-22 and cyclic RGD functionalized liposomes for glioma targeting drug delivery overcoming BBB and BBTB, ACS Appl. Mater. Interfaces 9 (7) (2017) 5864–5873.
[272] L. Han, et al., Targeted drug delivery to ischemic stroke via chlorotoxin-anchored, lexiscan-loaded nanoparticles, Nanomedicine 12 (7) (2016) 1833–1842.
[273] C. Zhang, et al., Direct macromolecular drug delivery to cerebral ischemia area using neutrophil-mediated nanoparticles, Theranostics 7 (13) (2017) 3260–3275.
[274] H. Yang, et al., pH-sensitive, cerebral vasculature-targeting hydroxyethyl starch functionalized nanoparticles for improved angiogenesis and neurological function recovery in ischemic stroke, Adv. Healthc. Mater. 10 (12) (2021) e2100028.
[275] Q. Song, et al., Biomimetic ApoE-reconstituted high density lipoprotein nanocarrier for blood-brain barrier penetration and amyloid beta-targeting drug delivery, Mol. Pharm. 13 (11) (2016) 3976–3987.
[276] K. Papadia, et al., Multifunctional LUV liposomes decorated for BBB and amyloid targeting - B. In vivo brain targeting potential in wild-type and APP/PS1 mice, Eur. J. Pharm. Sci. 102 (2017) 180–187.
[277] J. Sun, et al., Progressive release of mesoporous nano-selenium delivery system for the multi-channel synergistic treatment of Alzheimer's disease, Biomaterials 197 (2019) 417–431.
[278] C. Gao, et al., Neuronal mitochondria-targeted delivery of curcumin by biomimetic engineered nanosystems in Alzheimer's disease mice, Acta Biomater. 108 (2020) 285–299.
[279] C. Gao, et al., Neuron tau-targeting biomimetic nanoparticles for curcumin delivery to delay progression of Alzheimer's disease, J. Nanobiotechnol. 18 (1) (2020) 71.
[280] Y. Han, et al., Neuronal mitochondria-targeted therapy for Alzheimer's disease by systemic delivery of resveratrol using dual-modified novel biomimetic nanosystems, Drug Deliv. 27 (1) (2020) 502–518.
[281] Y. Han, et al., Macrophage membrane-coated nanocarriers Co-Modified by RVG29 and TPP improve brain neuronal mitochondria-targeting and therapeutic efficacy in Alzheimer's disease mice, Bioact. Mater. 6 (2) (2021) 529–542.
[282] X. Tao, et al., Brain-targeted polysorbate 80-emulsified donepezil drug-loaded nanoparticles for neuroprotection, Nanoscale Res. Lett. 16 (1) (2021) 132.
[283] J. Rao, A. Dragulescu-Andrasi, H. Yao, Fluorescence imaging in vivo: recent advances, Curr. Opin. Biotechnol. 18 (1) (2007) 17–25.
[284] R. Bouchaala, et al., Integrity of lipid nanocarriers in bloodstream and tumor quantified by near-infrared ratiometric FRET imaging in living mice, J. Control. Release 236 (2016) 57–67.
[285] F. Ding, et al., Beyond 1000 nm emission wavelength: recent advances in organic and inorganic emitters for deep-tissue molecular imaging, Adv. Healthc. Mater. 8 (14) (2019) 1900260.
[286] N.U. Khan, et al., Escape from abluminal LRP1-mediated clearance for boosted nanoparticle brain delivery and brain metastasis treatment, Acta Pharm. Sin. B 11 (5) (2021) 1341–1354.
[287] A. Ramanathan, et al., Impaired vascular-mediated clearance of brain amyloid beta in Alzheimer's disease: the role, regulation and restoration of LRP1, Front. Aging Neurosci. 7 (2015) 136.
[288] Y. Shi, et al., Boosting RNAi therapy for orthotopic glioblastoma with nontoxic brain-targeting chimaeric polymersomes, J. Control. Release 292 (2018) 163–171.
[289] Y. Jiang, et al., PEGylated Polyamidoamine dendrimer conjugated with tumor homing peptide as a potential targeted delivery system for glioma, Colloids Surf. B: Biointerfaces 147 (2016) 242–249.
[290] J. Hu, et al., Asn-Gly-Arg-modified polydopamine-coated nanoparticles for dual-targeting therapy of brain glioma in rats, Oncotarget 7 (45) (2016) 73681–73696.
[291] T. Lin, et al., Blood-brain-barrier-penetrating albumin nanoparticles for biomimetic drug delivery via albumin-binding protein pathways for antiglioma therapy, ACS Nano 10 (11) (2016) 9999–10012.
[292] H. Qin, et al., Oncoprotein inhibitor Rigosertib loaded in ApoE-targeted smart Polymersomes reveals high safety and potency against human glioblastoma in mice, Mol. Pharm. 16 (8) (2019) 3711–3719.
[293] J.L. Huang, et al., Lipoprotein-biomimetic nanostructure enables efficient targeting delivery of siRNA to Ras-activated glioblastoma cells via macropinocytosis, Nat. Commun. 8 (2017) 15144.
[294] Y. Zhao, et al., Dual targeted nanocarrier for brain ischemic stroke treatment, J. Control. Release 233 (2016) 64–71.
[295] N. Serna, et al., Rational engineering of single-chain polypeptides into protein-only, BBB-targeted nanoparticles, Nanomedicine 12 (5) (2016) 1241–1251.
[296] C. Dende, et al., Nanocurcumin is superior to native curcumin in preventing degenerative changes in experimental cerebral malaria, Sci. Rep. 7 (1) (2017) 10062.
[297] T. Yin, et al., Penetratin peptide-functionalized gold nanostars: enhanced BBB permeability and NIR photothermal treatment of Alzheimer's disease using ultralow irradiance, ACS Appl. Mater. Interfaces 8 (30) (2016) 19291–19302.
[298] Y. Xu, et al., Lactoferrin-coated polysaccharide nanoparticles based on chitosan hydrochloride/hyaluronic acid/PEG for treating brain glioma, Carbohydr. Polym. 157 (2017) 419–428.
[299] M. Xu, et al., Ultrasound-excited Protoporphyrin IX-modified multifunctional nanoparticles as a strong inhibitor of tau phosphorylation and beta-amyloid aggregation, ACS Appl. Mater. Interfaces 10 (39) (2018) 32965–32980.
[300] S. Lakkadwala, et al., Dual functionalized liposomes for efficient co-delivery of anti-cancer chemotherapeutics for the treatment of glioblastoma, J. Control. Release 307 (2019) 247–260.
[301] M. Petro, et al., Tissue plasminogen activator followed by antioxidant-loaded nanoparticle delivery promotes activation/mobilization of progenitor cells in infarcted rat brain, Biomaterials 81 (2016) 169–180.
[302] E. Sanchez-Lopez, et al., New potential strategies for Alzheimer's disease prevention: pegylated biodegradable dexibuprofen nanospheres administration to APPswe/PS1dE9, Nanomedicine 13 (3) (2017) 1171–1182.
[303] D. Gonzalez-Carter, et al., Targeting nanoparticles to the brain by exploiting the blood-brain barrier impermeability to selectively label the brain endothelium, Proc. Natl. Acad. Sci. USA 117 (32) (2020) 19141–19150.
[304] F.U. Amin, et al., Osmotin-loaded magnetic nanoparticles with electromagnetic guidance for the treatment of Alzheimer's disease, Nanoscale 9 (30) (2017) 10619–10632.
[305] P. Marcianes, et al., Surface-modified gatifloxacin nanoparticles with potential for treating central nervous system tuberculosis, Int. J. Nanomedicine 12 (2017) 1959–1968.
[306] X. Zheng, et al., Dual-functional nanoparticles for precise drug delivery to Alzheimer's disease lesions: targeting mechanisms, pharmacodynamics and safety, Int. J. Pharm. 525 (1) (2017) 237–248.
[307] D.X. Medina, et al., Optical barcoding of PLGA for multispectral analysis of nanoparticle fate in vivo, J. Control. Release 253 (2017) 172–182.
[308] C.K. Weiss, et al., The first step into the brain: uptake of NIO-PBCA nanoparticles by endothelial cells in vitro and in vivo, and direct evidence for their blood-brain barrier permeation, ChemMedChem 3 (9) (2008) 1395–1403.
[309] C. Zhang, et al., Strategies to enhance the distribution of nanotherapeutics in the brain, J. Control. Release 267 (2017) 232–239.
[310] L. Wang, et al., Intranasal delivery of Temozolomide-conjugated gold nanoparticles functionalized with anti-EphA3 for glioblastoma targeting, Mol. Pharm. 18 (3) (2021) 915–927.

[311] J.K. Saucier-Sawyer, et al., Distribution of polymer nanoparticles by convection-enhanced delivery to brain tumors, J. Control. Release 232 (2016) 103–112.
[312] W.G. Singleton, et al., Convection enhanced delivery of panobinostat (LBH589)-loaded pluronic nano-micelles prolongs survival in the F98 rat glioma model, Int. J. Nanomedicine 12 (2017) 1385–1399.
[313] Z. Sun, et al., Application of dual targeting drug delivery system for the improvement of anti-glioma efficacy of doxorubicin, Oncotarget 8 (35) (2017) 58823–58834.
[314] K. Mayilsamy, et al., Treatment with shCCL20-CCR6 nanodendriplexes and human mesenchymal stem cell therapy improves pathology in mice with repeated traumatic brain injury, Nanomedicine 29 (2020) 102247.
[315] J.H. Jeong, et al., Protective effect of Cholic acid-coated poly lactic-co-glycolic acid (PLGA) nanoparticles loaded with erythropoietin on experimental stroke, J. Nanosci. Nanotechnol. 19 (10) (2019) 6524–6533.
[316] M. Meenu, et al., Evaluation of sodium valproate loaded nanoparticles in acute and chronic pentylenetetrazole induced seizure models, Epilepsy Res. 158 (2019) 106219.
[317] E. Aso, et al., Poly(propylene imine) dendrimers with histidine-maltose shell as novel type of nanoparticles for synapse and memory protection, Nanomedicine 17 (2019) 198–209.
[318] A. Del Grosso, et al., Brain-targeted enzyme-loaded nanoparticles: a breach through the blood-brain barrier for enzyme replacement therapy in Krabbe disease, Sci. Adv. 5 (11) (2019) eaax7462.
[319] J.C. Grimm, et al., Nanotechnology approaches to targeting inflammation and excitotoxicity in a canine model of hypothermic circulatory arrest-induced brain injury, Ann. Thorac. Surg. 102 (3) (2016) 743–750.
[320] C. Portioli, et al., Novel functionalization strategies of polymeric nanoparticles as carriers for brain medications, J. Biomed. Mater. Res. A 105 (3) (2017) 847–858.
[321] R. Sharma, et al., Activated microglia targeting dendrimer-minocycline conjugate as therapeutics for Neuroinflammation, Bioconjug. Chem. 28 (11) (2017) 2874–2886.
[322] A.E. Aly, et al., Intranasal delivery of hGDNF plasmid DNA nanoparticles results in long-term and widespread transfection of perivascular cells in rat brain, Nanomedicine 16 (2019) 20–33.
[323] R. Sharma, et al., Dendrimer mediated targeted delivery of sinomenine for the treatment of acute neuroinflammation in traumatic brain injury, J. Control. Release 323 (2020) 361–375.
[324] L. Wen, et al., VEGF-mediated tight junctions pathological fenestration enhances doxorubicin-loaded glycolipid-like nanoparticles traversing BBB for glioblastoma-targeting therapy, Drug Deliv. 24 (1) (2017) 1843–1855.
[325] L. Han, et al., Increased nanoparticle delivery to brain tumors by autocatalytic priming for improved treatment and imaging, ACS Nano 10 (4) (2016) 4209–4218.
[326] J.H. Kang, J. Cho, Y.T. Ko, Investigation on the effect of nanoparticle size on the blood-brain tumour barrier permeability by in situ perfusion via internal carotid artery in mice, J. Drug Target. 27 (1) (2019) 103–110.
[327] G.P. Hoyos-Ceballos, et al., PLGA-PEG-ANG-2 nanoparticles for blood-brain barrier crossing: proof-of-concept study, Pharmaceutics 12 (1) (2020).
[328] T. Zhang, et al., Multitargeted nanoparticles deliver synergistic drugs across the blood-brain barrier to brain metastases of triple negative breast cancer cells and tumor-associated macrophages, Adv. Healthc. Mater. 8 (18) (2019) e1900543.
[329] G. Graverini, et al., Solid lipid nanoparticles for delivery of andrographolide across the blood-brain barrier: in vitro and in vivo evaluation, Colloids Surf. B: Biointerfaces 161 (2018) 302–313.
[330] M. Ayer, et al., T cell-mediated transport of polymer nanoparticles across the blood-brain barrier, Adv. Healthc. Mater. 10 (2) (2021) e2001375.
[331] A. Zybina, et al., Nanoparticle-based delivery of carbamazepine: a promising approach for the treatment of refractory epilepsy, Int. J. Pharm. 547 (1–2) (2018) 10–23.
[332] P. Moscariello, et al., Unraveling in vivo brain transport of protein-coated fluorescent nanodiamonds, Small 15 (42) (2019) e1902992.
[333] D.S. Jain, et al., Thermosensitive PLA based nanodispersion for targeting brain tumor via intranasal route, Mater. Sci. Eng. C Mater. Biol. Appl. 63 (2016) 411–421.
[334] F. Zhang, et al., Surface functionality affects the biodistribution and microglia-targeting of intra-amniotically delivered dendrimers, J. Control. Release 237 (2016) 61–70.
[335] Y. Zhang, et al., Transporter protein and drug-conjugated gold nanoparticles capable of bypassing the blood-brain barrier, Sci. Rep. 6 (2016) 25794.
[336] L.B. Thomsen, et al., Evaluation of targeted delivery to the brain using magnetic immunoliposomes and magnetic force, Materials (Basel) 12 (21) (2019).
[337] J.N. May, et al., Multimodal and multiscale optical imaging of nanomedicine delivery across the blood-brain barrier upon sonopermeation, Theranostics 10 (4) (2020) 1948–1959.
[338] A. Pascu, et al., Laser-induced autofluorescence measurements on brain tissues, Anat. Rec. (Hoboken) 292 (12) (2009) 2013–2022.
[339] J.L.A.N. Murk, et al., Endosomal compartmentalization in three dimensions: implications for membrane fusion, Proc. Natl. Acad. Sci. 100 (23) (2003) 13332–13337.
[340] Y.W. Jun, et al., Addressing the autofluorescence issue in deep tissue imaging by two-photon microscopy: the significance of far-red emitting dyes, Chem. Sci. 8 (11) (2017) 7696–7704.
[341] A.C. Croce, G. Bottiroli, Autofluorescence spectroscopy and imaging: a tool for biomedical research and diagnosis, Eur. J. Histochem. 58 (4) (2014) 2461.
[342] I. Khalin, et al., Dynamic tracing using ultra-bright labelling and multi-photon microscopy identifies endothelial uptake of poloxamer 188 coated poly(lactic-co-glycolic acid) nano-carriers in vivo, Nanomed.: Nanotechn. Biol. Med. 40 (2022) 102511.
[343] J. Xu, et al., Sequentially site-specific delivery of thrombolytics and neuroprotectant for enhanced treatment of ischemic stroke, ACS Nano 13 (8) (2019) 8577–8588.
[344] D. Sehedic, et al., Locoregional confinement and major clinical benefit of (188)re-loaded CXCR4-targeted nanocarriers in an orthotopic human to mouse model of glioblastoma, Theranostics 7 (18) (2017) 4517–4536.
[345] L.D. Lavis, R.T. Raines, Bright ideas for chemical biology, ACS Chem. Biol. 3 (3) (2008) 142–155.
[346] A.H. Ashoka, et al., Brightness of fluorescent organic nanomaterials, Chem. Soc. Rev. 52 (14) (2023) 4525–4548.
[347] O.S. Wolfbeis, An overview of nanoparticles commonly used in fluorescent bioimaging, Chem. Soc. Rev. 44 (14) (2015) 4743–4768.
[348] W.R. Algar, et al., Photoluminescent nanoparticles for chemical and biological analysis and imaging, Chem. Rev. 121 (15) (2021) 9243–9358.
[349] W.C.W. Chan, et al., Luminescent quantum dots for multiplexed biological detection and imaging, Curr. Opin. Biotechnol. 13 (1) (2002) 40–46.
[350] I.L. Medintz, et al., Quantum dot bioconjugates for imaging, labelling and sensing, Nat. Mater. 4 (6) (2005) 435–446.
[351] X. Michalet, et al., Quantum dots for live cells, in vivo imaging, and diagnostics, Science 307 (5709) (2005) 538–544.
[352] V.N. Mochalin, et al., The properties and applications of nanodiamonds, Nat. Nanotechnol. 7 (1) (2012) 11–23.
[353] S.-T. Yang, et al., Carbon dots for optical imaging in vivo, J. Am. Chem. Soc. 131 (32) (2009) 11308–11309.
[354] H.-S. Peng, D.T. Chiu, Soft fluorescent nanomaterials for biological and biomedical imaging, Chem. Soc. Rev. 44 (14) (2015) 4699–4722.
[355] A. Reisch, A.S. Klymchenko, Fluorescent polymer nanoparticles based on dyes: seeking brighter tools for bioimaging, Small 12 (15) (2016) 1968–1992.
[356] A.S. Klymchenko, et al., Dye-loaded nanoemulsions: biomimetic fluorescent nanocarriers for bioimaging and nanomedicine, Adv. Healthc. Mater. 10 (1) (2021) 2001289.
[357] I. Khalin, et al., Size-selective transfer of lipid nanoparticle-based drug carriers across the blood brain barrier via vascular occlusions following traumatic brain injury, Small 18 (18) (2022) e2200302.
[358] B. Andreiuk, et al., Fluorescent polymer nanoparticles for cell barcoding in vitro and in vivo, Small 13 (38) (2017) 1701582.
[359] J. Sobska, et al., Counterion-insulated near-infrared dyes in biodegradable polymer nanoparticles for in vivo imaging, Nanoscale Adv. 4 (1) (2022) 39–48.
[360] A. Reisch, et al., Collective fluorescence switching of counterion-assembled dyes in polymer nanoparticles, Nat. Commun. 5 (2014) 4089.
[361] A. Reisch, et al., Charge-controlled nanoprecipitation as a modular approach to ultrasmall polymer nanocarriers: making bright and stable nanoparticles, ACS Nano 9 (5) (2015) 5104–5116.
[362] V.N. Kilin, et al., Counterion-enhanced cyanine dye loading into lipid nano-droplets for single-particle tracking in zebrafish, Biomaterials 35 (18) (2014) 4950–4957.
[363] B. Andreiuk, et al., Fighting aggregation-caused quenching and leakage of dyes in fluorescent polymer nanoparticles: universal role of Counterion, Chem. Asian J. 14 (6) (2019) 836–846.
[364] R. Munter, et al., Dissociation of fluorescently labeled lipids from liposomes in biological environments challenges the interpretation of uptake studies, Nanoscale 10 (48) (2018) 22720–22724.
[365] A.S. Klymchenko, et al., Highly lipophilic fluorescent dyes in nano-emulsions: towards bright non-leaking nano-droplets, RSC Adv. 2 (31) (2012) 11876–11886.
[366] A.S. Klymchenko, et al., Dye-loaded nanoemulsions: biomimetic fluorescent nanocarriers for bioimaging and nanomedicine, Adv. Healthc. Mater. 10 (1) (2021) e2001289.
[367] R. Schubert, Liposome preparation by detergent removal, in: Methods in Enzymology, Academic Press, 2003, pp. 46–70.
[368] A. Hoffmann, et al., High and low molecular weight fluorescein isothiocyanate (FITC)–Dextrans to assess blood-brain barrier disruption: technical considerations, Transl. Stroke Res. 2 (1) (2011) 106–111.
[369] K. Cortese, A. Diaspro, C. Tacchetti, Advanced correlative light/electron microscopy: current methods and new developments using Tokuyasu cryosections, J. Histochem. Cytochem. 57 (12) (2009) 1103–1112.
[370] G.F. Georg Kislinger, Antonia Wehn, Lucia Rodriguez, Hanyi Jiang, Cornelia Niemann, Andrey S. Klymchenko, Nikolaus Plesnila, Thomas Misgeld, Thomas Müller-Reichert, Igor Khalin, Martina Schifferer, ATUM-Tomo: A multi-scale approach to cellular ultrastructure by combined volume scanning electron microscopy and electron tomography, eLife (2023), https://doi.org/10.7554/eLife.90565.1 (Preprint).
[371] S. Hayashi, et al., Correlative light and volume electron microscopy to study brain development, Microscopy (Oxf) 72 (4) (2023) 279–286.
[372] Y.W. Choo, J. Jeong, K. Jung, Recent advances in intravital microscopy for investigation of dynamic cellular behavior in vivo, BMB Rep. 53 (7) (2020) 357–366.
[373] X. Deng, M. Gu, Penetration depth of single-, two-, and three-photon fluorescence microscopic imaging through human cortex structures: Monte Carlo simulation, Appl. Opt. 42 (16) (2003) 3321–3329.
[374] J.M. Rabanel, et al., Transport of PEGylated-PLA nanoparticles across a blood brain barrier model, entry into neuronal cells and in vivo brain bioavailability, J. Control. Release 328 (2020) 679–695.

[375] L. Chen, et al., Improving the delivery of SOD1 antisense oligonucleotides to motor neurons using calcium phosphate-lipid nanoparticles, Front. Neurosci. 11 (2017) 476.
[376] J. Condeelis, R. Weissleder, In vivo imaging in cancer, Cold Spring Harb. Perspect. Biol. 2 (12) (2010) a003848.
[377] D. Entenberg, et al., Setup and use of a two-laser multiphoton microscope for multichannel intravital fluorescence imaging, Nat. Protoc. 6 (10) (2011) 1500–1520.
[378] P. Pantazis, et al., Second harmonic generating (SHG) nanoprobes for in vivo imaging, Proc. Natl. Acad. Sci. USA 107 (33) (2010) 14535–14540.
[379] H. Baghirov, et al., Feasibility study of the permeability and uptake of mesoporous silica nanoparticles across the blood-brain barrier, PLoS One 11 (8) (2016) e0160705.
[380] A. Zinger, et al., Biomimetic nanoparticles as a theranostic tool for traumatic brain injury, Adv. Funct. Mater. 31 (30) (2021) 2100722.
[381] Z.S. Al-Ahmady, et al., Selective liposomal transport through blood brain barrier disruption in ischemic stroke reveals two distinct therapeutic opportunities, ACS Nano 13 (11) (2019) 12470–12486.
[382] K. Kucharz, et al., Post-capillary venules are the key locus for transcytosis-mediated brain delivery of therapeutic nanoparticles, Nat. Commun. 12 (1) (2021) 4121.
[383] Y. Anraku, et al., Glycaemic control boosts glucosylated nanocarrier crossing the BBB into the brain, Nat. Commun. 8 (1) (2017) 1001.
[384] S. Yang, et al., Anesthesia and surgery impair blood-brain barrier and cognitive function in mice, Front. Immunol. 8 (2017) 902.
[385] J. Icha, et al., Phototoxicity in live fluorescence microscopy, and how to avoid it. BioEssays: news and reviews in molecular, Cell. Develop. Biol. 39 (8) (2017).
[386] S.F. Rodrigues, et al., Lipid-Core Nanocapsules act as a drug shuttle through the blood brain barrier and reduce glioblastoma after intravenous or Oral administration, J. Biomed. Nanotechnol. 12 (5) (2016) 986–1000.
[387] Y.-J. Zhao, et al., Skull optical clearing window for in vivo imaging of the mouse cortex at synaptic resolution, Light: Sci. Appl. 7 (2) (2018) 17153.
[388] D. Li, et al., AIE-nanoparticle assisted ultra-deep three-photon microscopy in the in vivo mouse brain under 1300 nm excitation, Mater. Chem. Front. 5 (7) (2021) 3201–3208.
[389] P. Wu, L. Brand, Resonance energy transfer: methods and applications, Anal. Biochem. 218 (1) (1994) 1–13.
[390] N.T. Chen, et al., Recent advances in nanoparticle-based Forster resonance energy transfer for biosensing, molecular imaging and drug release profiling, Int. J. Mol. Sci. 13 (12) (2012) 16598–16623.
[391] J. Shi, et al., Nanoparticle based fluorescence resonance energy transfer (FRET) for biosensing applications, J. Mater. Chem. B 3 (35) (2015) 6989–7005.
[392] J.E. Tengood, et al., Real-time analysis of composite magnetic nanoparticle disassembly in vascular cells and biomimetic media, Proc. Natl. Acad. Sci. USA 111 (11) (2014) 4245–4250.
[393] S.W. Morton, et al., FRET-enabled biological characterization of polymeric micelles, Biomaterials 35 (11) (2014) 3489–3496.
[394] Y. Li, et al., Zebrafish as a visual and dynamic model to study the transport of nanosized drug delivery systems across the biological barriers, Colloids Surf. B: Biointerfaces 156 (2017) 227–235.
[395] J. Peng, et al., High-efficiency in vitro and in vivo detection of Zn2+ by dye-assembled upconversion nanoparticles, J. Am. Chem. Soc. 137 (6) (2015) 2336–2342.
[396] T. Chen, et al., Small-sized mPEG-PLGA nanoparticles of Schisantherin a with sustained release for enhanced brain uptake and anti-parkinsonian activity, ACS Appl. Mater. Interfaces 9 (11) (2017) 9516–9527.
[397] W. Liu, et al., Fluorescence resonance energy transfer (FRET) based nanoparticles composed of AIE luminogens and NIR dyes with enhanced three-photon near-infrared emission for in vivo brain angiography, Nanoscale 10 (21) (2018) 10025–10032.
[398] T. Chen, et al., Nanoparticles mediating the sustained Puerarin release facilitate improved brain delivery to treat Parkinson's disease, ACS Appl. Mater. Interfaces 11 (48) (2019) 45276–45289.
[399] C. Li, et al., Protein nanoparticle-related osmotic pressure modifies nonselective permeability of the blood-brain barrier by increasing membrane fluidity, Int. J. Nanomedicine 16 (2021) 1663–1680.
[400] X. Ye, et al., FRET modulated signaling: a versatile strategy to construct Photoelectrochemical microsensors for in vivo analysis, Angew. Chem. Int. Ed. Eng. 60 (21) (2021) 11774–11778.
[401] Energy Transfer, in: J.R. Lakowicz (Ed.), Principles of Fluorescence Spectroscopy, Springer US, Boston, MA, 2006, pp. 443–475.
[402] F.W. Pratiwi, et al., Recent advances in the use of fluorescent nanoparticles for bioimaging, Nanomedicine (London) 14 (13) (2019) 1759–1769.
[403] Q. Lin, P. Fathi, X. Chen, Nanoparticle delivery in vivo: A fresh look from intravital imaging, eBioMedicine (2020) 59.
[404] A.K. Pearce, R.K. O'Reilly, Insights into active targeting of nanoparticles in drug delivery: advances in clinical studies and design considerations for cancer nanomedicine, Bioconjug. Chem. 30 (9) (2019) 2300–2311.
[405] M.C. Mendonca, et al., Reduced graphene oxide: nanotoxicological profile in rats, J. Nanobiotechnol. 14 (1) (2016) 53.
[406] A. Kowalik, et al., Dopamine D(2) and serotonin 5-HT(1A) dimeric receptor-binding monomeric antibody scFv as a potential ligand for carrying drugs targeting selected areas of the brain, Biomolecules 12 (6) (2022).
[407] S.T. Chou, et al., Simultaneous blockade of interacting CK2 and EGFR pathways by tumor-targeting nanobioconjugates increases therapeutic efficacy against glioblastoma multiforme, J. Control. Release 244 (Pt A) (2016) 14–23.
[408] E. Sekerdag, et al., A potential non-invasive glioblastoma treatment: nose-to-brain delivery of farnesylthiosalicylic acid incorporated hybrid nanoparticles, J. Control. Release 261 (2017) 187–198.
[409] Y. Zhang, et al., Versatile metal-phenolic network nanoparticles for multitargeted combination therapy and magnetic resonance tracing in glioblastoma, Biomaterials 278 (2021) 121163.
[410] S. Thirumurugan, et al., Angiopep-2-decorated titanium-alloy core-shell magnetic nanoparticles for nanotheranostics and medical imaging, Nanoscale 14 (39) (2022) 14789–14800.
[411] Z.S. Al-Ahmady, et al., Selective brain entry of lipid nanoparticles in haemorrhagic stroke is linked to biphasic blood-brain barrier disruption, Theranostics 12 (10) (2022) 4477–4497.
[412] R. Zhou, et al., Targeted brain delivery of RVG29-modified rifampicin-loaded nanoparticles for Alzheimer's disease treatment and diagnosis, Bioeng. Transl. Med. 7 (3) (2022) e10395.
[413] L.J. Cruz, et al., Effect of PLGA NP size on efficiency to target traumatic brain injury, J. Control. Release 223 (2016) 31–41.
[414] T.I. Janjua, et al., Efficient delivery of Temozolomide using ultrasmall large-pore silica nanoparticles for glioblastoma, J. Control. Release 357 (2023) 161–174.
[415] L. Dong, et al., A Gambogic acid-loaded delivery system mediated by ultrasound-targeted microbubble destruction: a promising therapy method for malignant cerebral glioma, Int. J. Nanomedicine 17 (2022) 2001–2017.
[416] T.G. Chan, et al., Targeted delivery of DNA-au nanoparticles across the blood-brain barrier using focused ultrasound, ChemMedChem 13 (13) (2018) 1311–1314.
[417] S. Blanco, et al., Hyaluronate nanoparticles as a delivery system to carry neuroglobin to the brain after stroke, Pharmaceutics 12 (1) (2020).
[418] H. Li, et al., Angiopep-2 modified exosomes load rifampicin with potential for treating central nervous system tuberculosis, Int. J. Nanomedicine 18 (2023) 489–503.